1988

An experimental study of selected face ventilation parameters and their effect on respirable coal-dust dispersion.

Tzuu Hsing Ueng

Order Number 9001115

An experimental study of selected face ventilation parameters and their effect on respirable coal dust dispersion

Ueng, Tzuu Hsing, Ph.D.

West Virginia University, 1988

U·M·I
300 N. Zeeb Rd.
Ann Arbor, MI 48106

AN EXPERIMENTAL STUDY OF SELECTED FACE VENTILATION PARAMETERS AND THEIR EFFECT ON RESPIRABLE COAL DUST DISPERSION

by

Tzuu Hsing Ueng

A Dissertation

Submitted to the Faculty of

Department of Mining Engineering

College of Mineral and Energy Resources

West Virginia University

In Partial Fulfillment of the Requirements

for the Degree of

Doctor of Philosophy

in

Mining Engineering

Morgantown, West Virginia

March 1988

AN EXPERIMENTAL STUDY OF SELECTED FACE VENTILATION PARAMETERS AND THEIR EFFECT ON RESPIRABLE COAL DUST DISPERSION

Ueng,Tzuu Hsing West Virginia University, 1988. 120pp.

Mine face ventilation is generally regarded as the most effective tool for lowering the concentrations of respirable dust. A practical and economical way to gain more in-depth understanding of the relationship between mine face ventilation and dust dispersion is through scale model studies. Researchers have established that the results of these studies can be scaled-up as long as geometric, kinematic, and dynamic similitudes exist between the scale model and the full scale system.

To better understand face ventilation and dust dispersion, a one-fifth scale model of room and pillar mine face was constructed. The model was then used to study the effects that line brattice distance (from the face) and air quantity had on dust dispersion. Sixteen combinations of brattice distances and air quantities were examined. The experiments utilized both methane and Arizona Road Dust for simulating the respirable coal dust. Methane or Road Dust concentrations were measured at 25 grid points for each brattice distance and air quantity combination. The tests were first carried out without face machines and the same conditions were repeated with the presence of face machines.

Upon completion of the experiments the data were summarized and compared. Rates of reductions in methane or Road Dust concentration because of increased air quantities or brattice extensions were calculated. In addition, concentration isopachs were drawn to observe the trend of changes in concentration pattern. Differences between the dust simulation substances and the presence of face machines were also discussed. The correlation between the ventilation parameters and dust simulators was examined at each grid point. Also, the statistical functions for predicting the dust concentration at each grid point from different simulating substances were also constructed by using regression techniques.

Recommendations were made in regard to controlling dust dispersion through increasing air quantity or extending line brattice. Consideration of face areas typically of high and low dust concentration was also recommended.

ABSTRACT

Mine face ventilation is generally regarded as the most effective tool for lowering the concentrations of respirable dust. A practical and economical way to gain more in-depth understanding of the relationship between mine face ventilation and dust dispersion is through scale model studies. Researchers have established that the results of these studies can be scaled-up as long as geometric, kinematic, and dynamic similitudes exist between the scale model and the full scale system.

To better understand face ventilation and dust dispersion, a one-fifth scale model of room and pillar mine face was constructed. The model was then used to study the effects that line brattice distance (from the face) and air quantity had on dust dispersion. Sixteen combinations of brattice distances and air quantities were examined. The experiments utilized both methane and Arizona Road Dust for simulating the respirable coal dust. Methane or Road Dust concentrations were measured at 25 grid points for each brattice distance and air quantity combination. The tests were first carried out without face machines and the same conditions were repeated with the presence of face machines.

Upon completion of the experiments the data were summarized and compared. Rates of reductions in methane or Road Dust concentration because of increased air quantities or brattice extensions were calculated. In addition, concentration isopachs were drawn to observe the trend of changes in concentration pattern. Differences between the dust simulation substances and the presence of face machines were also discussed. The correlation between the ventilation parameters and dust simulators was examined at each grid point. Also, the statistical functions for predicting the dust concentration at each grid point from different simulating substances were also constructed by using regression techniques.

Recommendations were made in regard to controlling dust dispersion through increasing air quantity or extending line brattice. Consideration of face areas typically of high and low dust concentration was also recommended.

ACKNOWLEDGMENTS

For their interest and support in this study, the author wishes to thank each examining and advisory committee member: Dr. R. N. Eli, Dr. W. A. Iskander, Dr. S. S. Peng, Dr. R. R. Rollins and Dr. Y. J. Wang. Special appreciation is extended to the committee chairman, Dr. Y. J. Wang, for his guidance and in the preparation of this dissertation. Also, the Department of Mining Engineering of West Virginia University is acknowledged for the financial support.

Thanks is also extended to Dr. J. L. Chang, Dr. J. K. Lee, and Dr. D. S. Thompson for their help and suggestions in constructing the scale model and conducting experiments.

Special thanks and appreciation are given to the author's family; without their encouragement, certainly this work would not have been finished.

This project has been supported by the Department of the Interior's Mineral Institutes program administered by the Bureau of Mines under allotment grant number G1135142.

TABLE OF CONTENTS

LIST OF TABLES

LIST OF FIGURES

Chapter 1

Introduction

1.1. Respirable Coal Dust

Respirable dust in coal mines has been considered as one of the major cause for coal miner pneumoconiosis, which not only causes agonizing pain to the patients and their family but also costs the companies and government billions of dollars. The Code of Federal Regulations (Anon., 1980) requires that the average concentration of airborne respirable dust during each shift to which a miner is exposed be no more than two milligrams per cubic meter. There is considerable interest among government agencies and mining related companies in investigating methods of controlling the generation and dispersion of respirable coal dust.

1.2. Ventilation Parameters and Scale Modeling

Mine face ventilation has been generally used for lowering the concentrations of respirable dust around the working face. The most commonly used method is directing fresh air to the face with line brattice. The fresh air sweeps the dust from the face and pushes it to the return side of the entry. Therefore, air quantity and location of the line brattice are the two most important face ventilation parameters. A limited amount of research has been undertaken to determine the relationships between these two parameters and the dust dispersion patterns. If these relationships are better understood, more efficient ways of controlling dust generation and dispersion may be evident.

A practical and economical way to gain more in-depth understanding of these relationships is through scale model studies. Scale modeling has been successfully used in the aerospace industry in solving dynamic problems. The modeling study permits more precise and repeatable control of parameters than full scale testing. Hence, scale modeling appears attractive for examining underground mine face ventilation problems. Past research (Gillies, 1986; Breslin and Strazisar, 1976; Stein et al., 1974) has shown that scale models can be successfully used in studying ventilation parameters provided that geometric, kinematic, and dynamic similitudes are maintained. However, in most of the previous works, methane was employed to simulate dust. The dust concentrations were only measured at a few locations. The effects of overall face dust dispersion caused by the change of ventilation parameters remains unclear. Also, no study has used methane and dust as dust simulators under the same setup to observe the similarity between methane and dust concentration patterns.

1.3. Purpose

From the literature review, it is apparent that a more in-depth study on the dust dispersion around the face area is needed. Such a study is needed to provide more information for controlling dust concentrations. The objective of this research is to observe the effects of different line brattice locations and changes of air quantities on dust dispersion. Also the combined effects of line brattice and air quantity on overall face dust concentration was also examined.

The same tests are conducted with, as well as without, the mine face machines being present. The effects on dust concentration patterns due to face machines was thereby examined. Comparisons were also made between the dust dispersion patterns for the two dust simulators (methane and dust). By using statistical methods, the correlation coefficients between the parameters and the concentration of dust simulators are also studied. Finally, the prediction functions for dust concentration at each grid point are constructed by using regression techniques.

Chapter 2

Literature Review

2.1. Ventilation Parameters and Dust Control

A literature review reveals that many factors effect the dispersion of respirable coal dust in a coal mine. Only those concerned with face ventilation are discussed below.

Line Brattice. Line brattice is the most widely used means of face ventilation in the room and pillar mining system. In the exhaust line brattice system, a line brattice is installed so as to deliver fresh air to the working face at a lower velocity. The air is directed over the mining machines and the operators, and then leaves the face behind the curtain at a higher velocity. As the air leaves the face behind the line brattice, it carries the contaminants away from the face. In the blowing system, the line brattice forces the air into other working faces at a higher velocity. It is coursed over the mining machines and the operators at a higher velocity and then is directed away from the face at a lower velocity.

The effectiveness of the line brattice is dependent, in part, on the distance between the end of the line brattice and the face. Its effectiveness also depends on the distance between the brattice and the tight rib. Past field studies (Mundell and Ondry, 1975) and scale model works (Stein et al., 1974; Breslin and Strazisar, 1976) suggest that the end of the line brattice should be within about ten feet of the face. This apparently results in the best dust control. It has also been suggested that the distance from the brattice to the tight rib should be about one third of the opening width. It should be pointed out that all the comparisons are made only at the positions of the operator while the effect on the dust concentration over the face area due to the change of brattice remains unclear.

Air Quantity. It is known that an increase in air quantity reduces the dust concentration by dilution. However, when the air velocity becomes too high, an appreciable amount of dust is picked up by the air stream and overcomes the effect of dilution. Since air velocities are relatively low in the room and pillar face, this effect is not likely to occur. In the room and pillar mining system, increasing the quantity of main air results in lower dust concentrations, but the extent of these reductions depends on the distance between the end of the brattice and the face (Stein et al., 1974).

In the longwall mining system, the air velocity is an important factor for lowering dust concentration. Based on the air measurements made at the longwall faces, Hall (1956) suggested the air velocity of about three hundred feet per minute. Generally, it is agreed that the air velocity should be around three to four hundred feet per minute to pick up the dust. However, according to a wind tunnel study (Holdkinson,1960), no appreciable airborne dust is generated unless the air velocity is greater than one thousand feet per minute.

2.2. Scale Modeling

Scale modeling had been successfully used in the study of aerodynamic problems. The merit of scale modeling in the study of coal mine ventilation and respirable dust control parameters is economics. Scale modeling is less expensive and also less time consuming than field studies. It also permits more precise and reproducible control of ventilation parameters. Flow patterns and transport of respirable dust in a scale model mine will be similar to those in a full scale mine if geometric, kinematic, and dynamic similitudes are maintained (Murphy, 1951). A model mine is geometrically similar to the full scale mine if a single scale ratio exists between the corresponding length in each system. Dynamic similitude requires a single scale ratio between inertial and viscous forces acting at corresponding points in the two systems. This can be achieved by maintaining the same Reynolds number for the flow in the model and the mine. Kinematic similitude requires that the velocities of all solid objects in both systems has a single scale ratio (Stein et al., 1974). Since it is difficult to generate respirable dust at a high controlled rate and to make accurate real-time dust measurements, other material such as methane gas is generally used to simulated dust in the scale modeling studies. In the early sixties, water and polystyrene spheres were used to simulate the ventilation at the face of a heading (Shuttleworth, 1964).

Chapter 3

Experimental Apparatus

3.1. Scale Model

A one-fifth scale model of room and pillar mining face was constructed to conduct the investigation. The complete experimental setup is shown in Figure 3.1, which consisted of a blower, a one-fifth scale continuous miner, a one-fifth scale shuttle car, a duct system, and dust simulators.

Duct System. The one-fifth scale model used in this study was designed and constructed out of heating ducts made of 20 gauge sheet metal. The system consisted of an elbow, a four-way tee, five four-foot joints, two four-foot joints with plexiglass view window on the top, and a transition element for a Dayton Fan (blower). The duct system was geometrically similar to a full scale mine entry of 7.5 ft by 20 ft.

Fan. In order to induce adequate air quantity into the duct system, a 24.5-inch Dayton centrifugal by Dayton Electric Manufacturing Company was connected to the duct system. This fan,

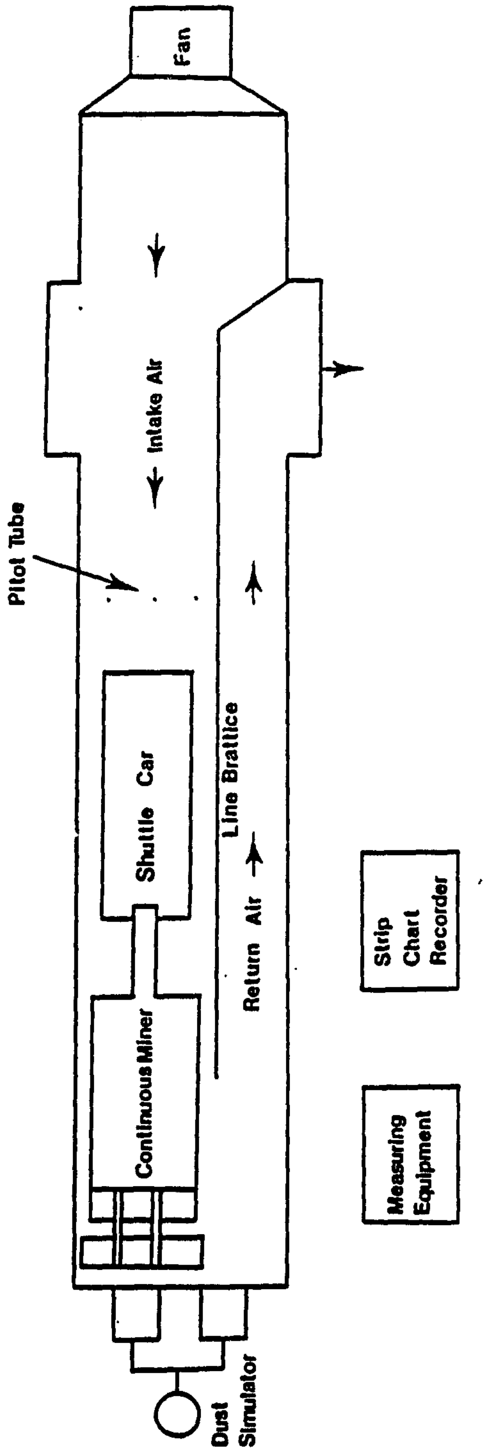

Fig. 3.1. Experimental Setup

operating under 115 volts, was capable of delivering 6000 cfm into the system. The air quantity was adjusted through changing the inlet area.

Line Brattice and Air Quantity. The duct system was divided by sheet metal to simulate the line brattice at one third width of the entry. The sheet metal was bolted to the duct and was sealed with duct tape. No apparent leakage was observed, therefore it was assumed to be minimal. Four brattice distances (i.e., the distance from the end of brattice to the face), representing full scale mine distances of 20, 15, 10, and 5 ft, were employed in the study. The air quantity was calculated from the velocity heads measured by a pitot tube at the intake airway. The data for velocity heads were further checked by using a hot wire anemometer at the same duct cross section. Four different air quantities were used in the tests, which represented the mine air quantities of 17,000, 12,000, 9,000, and 5,000 cfm.

Measuring Points. In order to measure the concentrations of the dust simulators and the air velocities across the face area, 25 holes in a grid arrangement were drilled on the top of the duct at the face area. The spacing and arrangement of the grid points are shown in Figure 3.2. Each hole was kept sealed unless a measurement was being taken at its location.

Injection Points. As shown in Figure 3.3, the end plate which covered the front of the heating duct had four small holes through which the dust simulators were injected.

Face Machine Models. One-fifth scale models of the continuous miner and the shuttle car were placed in the face area to simulate the face machines. They were built with 1/8-inch thick steel plate according to the size of Joy 14CM miner and Joy 21 SC shuttle car. The drum of the miner model rotated at 1500 rpm. It was also equipped with spiral bits. The dimensions of the machine models are given in Figures 3.4. and 3.5.

3.2. Substance Generators

Both methane gas and Arizona Road Dust (AC Spark Plug Div., General Motors Corporation, undated) were used to simulate respirable coal dust in the experiments. Each substance utilized its own generating mechanism.

Methane Gas. Methane was injected into the model from a 200 cubic foot pressurized cylinder. An Airco two stage regulator (Airco Industrial Gases, 1985) and an Airco flow meter were used

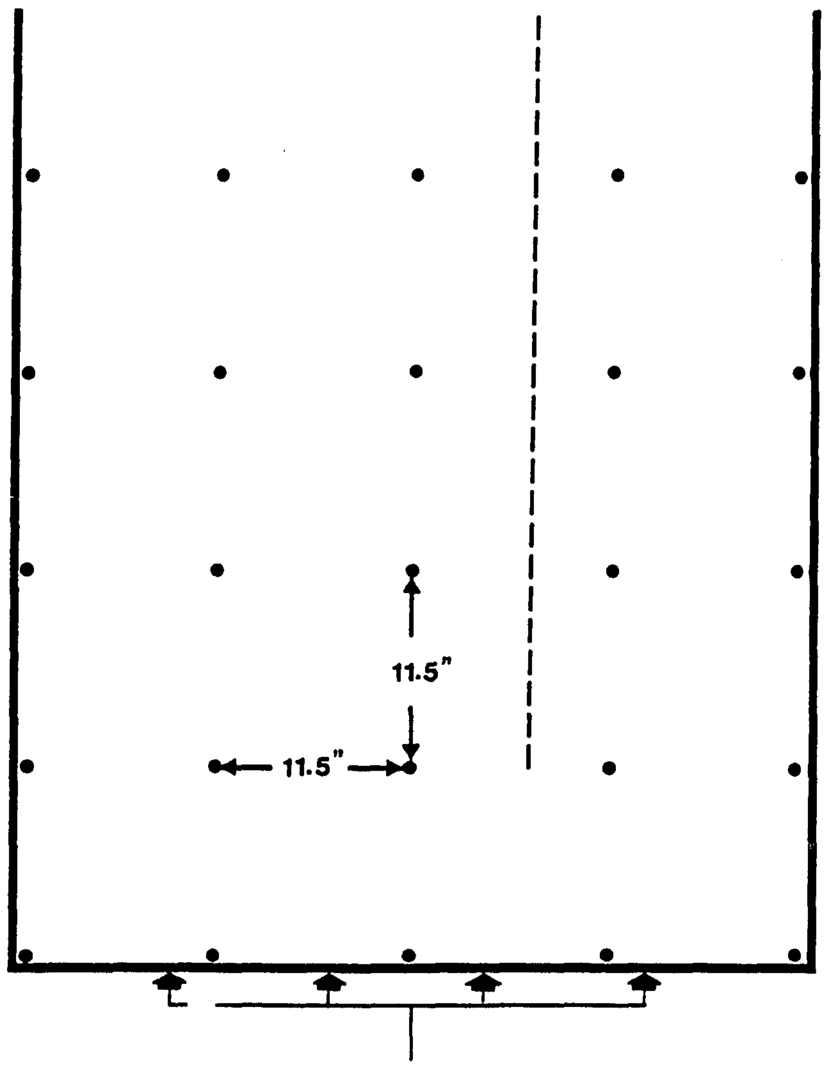

Fig. 3.2. Grid Points Arrangement

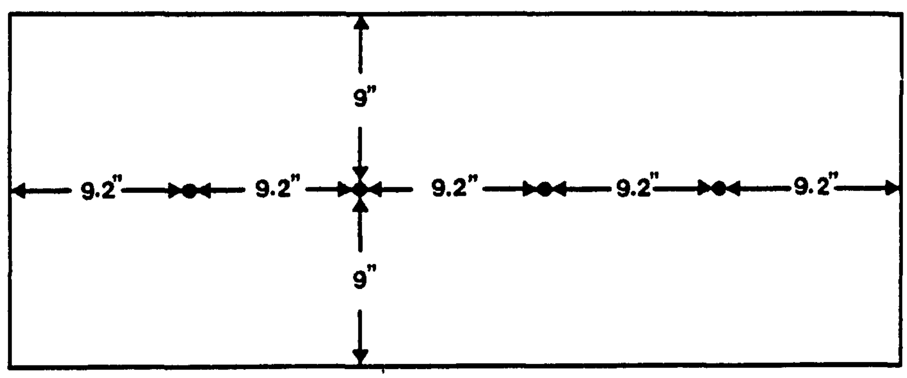

Fig. 3.3. Spacing of Injection Points

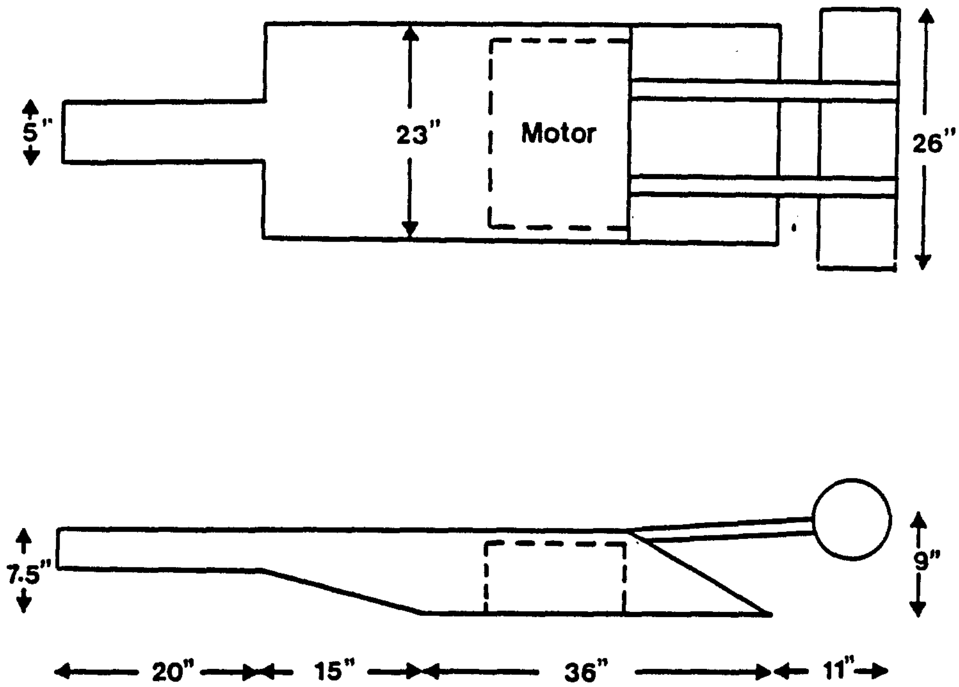

Fig. 3.4. Sketch of Continuous Miner Model

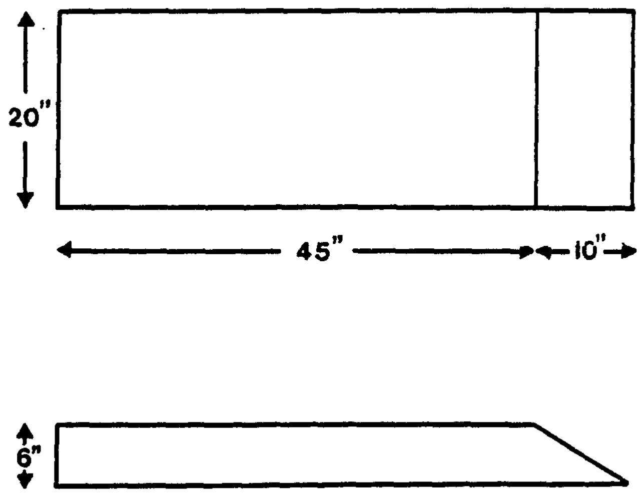

Fig. 3.5. Sketch of Shuttle Car Model

to ensure a constant feed of methane from the gas cylinder into the duct system.

Mark IX SYLCO Fine Powder Feeding Unit. The Arizona Road Dust was injected into the model by a Mark IX SYLCO Fine Powder Feeding Unit (Sylvester and Company, 1974) with compressed air as a carrier gas.

The powder feeding machine was manufactured by Sylvester and Company of Beachwood, Ohio. The feeding machine consisted of a sealed powder container and a variable speed screw assembly which was mounted on a electromagnetic vibrator. The screw entered the sealed powder container through a special packing gland located at the drive end and emerged on the other side of the container where it terminated in a carburetor. The carburetor mixed the powder with the carrier gas stream. The machine was designed to operate with a carrier gas only.

A variable speed screw driving mechanism was utilized to provide a controlled rate of powder feed and two different mixing chambers were incorporated in the apparatus to insure uniform mixing of the fine powders with the gas.

To prevent segregation of powder particles of various sizes and shapes, a special vibratory action was imparted to the powder canister by means of the electromagnetic vibrator located beneath it. The amplitude of the vibration could be controlled to suit various powder sizes and specific gravities. The vibratory action was designed to provide a slow boiling motion to the powder within the canister so there was no bridging and a constant turnover would take place.

Compressed air was used as a carrier gas throughout the tests. The air released pressure was set at 30 psi and the feeding screw speed was set at 50 rpm throughout the tests.

Arizona Road Dust. The Arizona Road Dust has been widely used in aerodynamic and air cleaner tests. The Road Dust used in this study was classified from natural Arizona dust. It was packed in a plastic jar with a net weight of ten pounds per jar. The particle size distributions, which were provided by the GM Corporation, is given in Tables 3.1 and 3.2. About twenty percent of the dust was under 10 micrometers.

3.3. Measuring Equipment

The methane concentrations, in parts per million (ppm), were measured with a Total Hydrocarbon Analyzer (Combustion Engineering, 1974), whereas the Road dust concentrations, in

Table 3.1. L & N Microtrac Coarse Dust Specification*

Microns	% smaller than
5.5	13 ± 3
11.0	24 ± 3
22.0	37 ± 3
44.0	56 ± 3
88.0	84 ± 3
176.0	100

* Provided by AC Spark Plug Div.., General Motors Corporation.

Table 3.2. Size Distribution of Arizona Road Dust*

Channel Upper Limit, microns	Cumulative Data % Smaller Than Channel Upper Limit	% Difference Between Channel and Next Smaller Channel
176.0	100.0	4.7
125.0	95.2	13.2
88.0	81.9	12.7
62.0	69.2	12.3
44.0	56.8	12.3
31.0	44.4	8.9
22.0	35.5	6.7
16.0	28.8	6.0
11.0	22.7	4.3
7.8	18.4	3.4
5.5	14.9	5.0
3.9	9.8	4.5
2.8	5.3	5.3

* Provided by AC Spark Plug Div.., General Motors Corporation

milligrams per cubic meter, were measured with a Real-Time Aerosol Monitor (GCA Corporation, 1979). The readings obtained from these two instruments were recorded with a Linear strip chart recorder. The air velocity head was measured by a pitot tube and checked with a hot wire anemometer at the cross section of the intake airway.

Total Hydrocarbon Analyzer. Methane concentration at each grid point was measured with a Total Hydrocarbon Analyzer (model 8401). The Analyzer uses a flame ionization detector (FID) to measure the concentration of hydrocarbon in the sample. It was designed to measure all hydrocarbon in a continuously exchanged ambient air sample. The Analyzer was equipped with a sampling pump which operated at 6.5 psig and 35 cc/min. It was also provided with the front panel recorder jacks and the rear panel terminals in addition to the front panel meter indicator.

The equipment was capable of detecting the methane concentration in the range of 1 to 100,000 ppm. Prior to the starting of experiments, the Analyzer was brought back to the factory for mechanical checking and for calibrating with zero gas and span gas. The installation of the analyzer is shown in Figure 3.6. Throughout the experiments, the hydrogen and air pressure were kept at 16 and 20.5 psig, respectively.

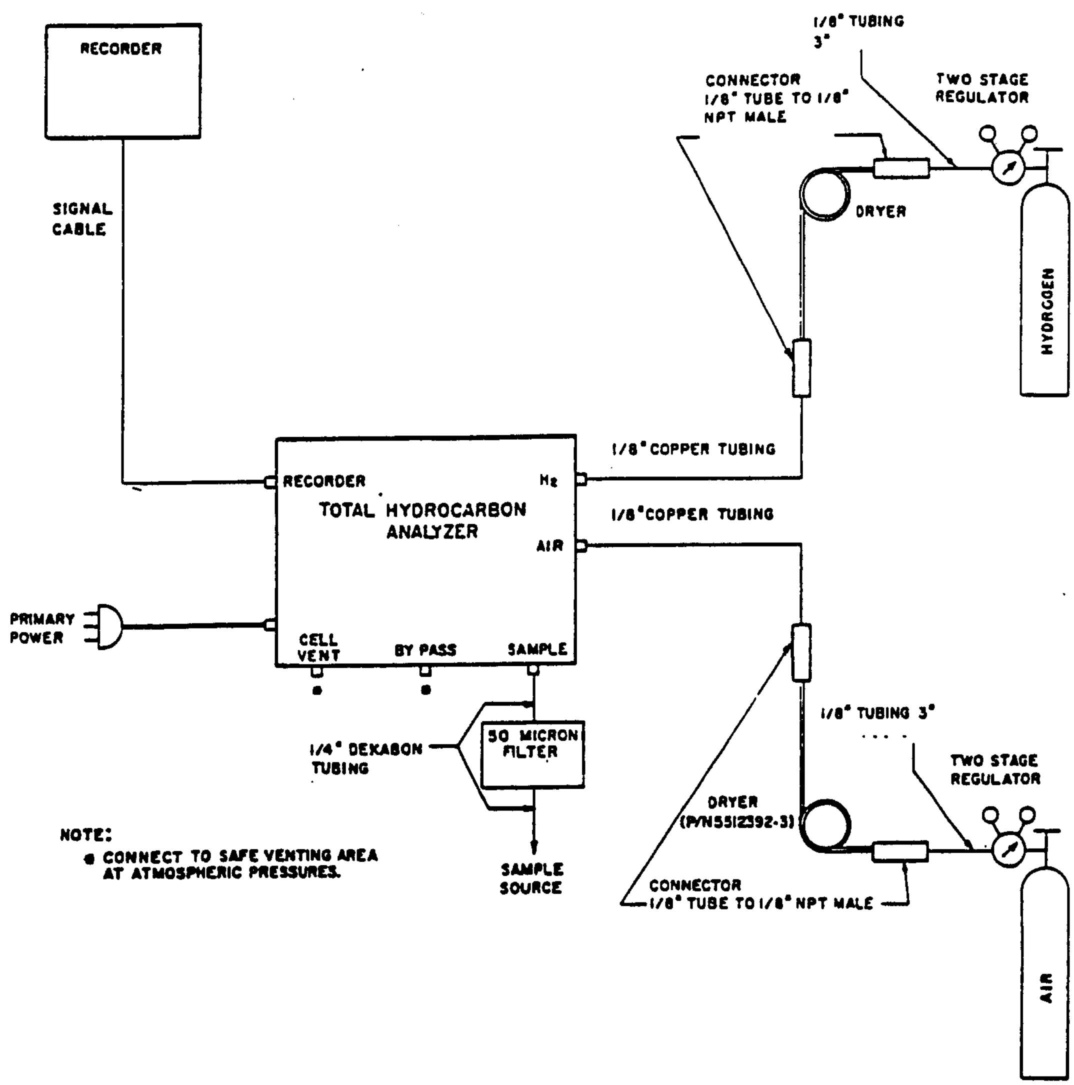

Fig. 3.8. Typical Layout of the Hydrocarbon Analyzer

Real-Time Aerosol Monitor. A Real-Time Aerosol Monitor (RAM-1) was used to measure the dust concentration at each grid point in the road dust tests. The monitor was built by GCA Corporation's Technology Division of Bedford, Massachusetts. The equipment utilized a pulsed light-emitting diode in combination with a silicon detector to sense the light scattered over a forward angle of 45 to 95 degrees by the particles traversing the sensing volume. The measurement range of the monitor was from 0.001 to 200 milligrams per cubic meter. The continuous readout was provided by a visible liquid crystal digital display. In addition to the digital display, a high level analog output signal was available for the direct operation of a strip chart recorder and/or for remote readout, recording, or process control applications.

Strip Chart Recorder. A Linear multiple channel strip chart recorder was used to record the readout obtained from both methane and dust tests. The recorder was built by Linear Instruments Corporation of Reno, Nevada. The range of the input signal voltage was 1 millivolt to 5 volts. The chart speed was adjustable within a range of 1 cm/hr to 30 cm/min. In both methane and dust testing, the chart speed was set at 2 cm/min.

<u>Hot Wire Anemometer.</u> A Dwyer Thermal Anemometer Series 470 (DAVIS Instrument Manufacturing Company, Inc., 1985) was used to measure the air velocity at the cross section of the intake airway as well as the air velocity across the working face area. The anemometer was a two stage meter with a lower range of zero to six hundred feet per minute and a higher range of five hundred to six thousand feet per minute. The accuracy of the measurement was ±5% full scale. The anemometer was automatic temperature compensated from 32 to 180 F.

Chapter 4

Procedure

To better understand the relationship between face ventilation parameters and dust dispersion, the one-fifth scale model was used to conduct experiments under various combinations of brattice locations and air quantities. The experiments were first carried out without face machines present. Methane was initially used as a dust simulator in every test, and then the same tests were repeated by using Arizona road dust for simulating the coal dust. Also, the changes in air velocity across the working area, caused by the change of air quantity and brattice extension, were also examined. Same tests were repeated with face machines present. A total of 64 tests were accomplished.

4.1. Line Brattice Distances

Throughout the study, the line brattice was set at one third of the width of the entry from the tight rib (Fig. 4.1). For the line brattice distance (i.e., the distance from the end of the line brattice to the face) four settings were employed in the study. They were 4, 3, 2, and 1 ft, corresponding to full scale distances of 20, 15, 10, and 5 ft, respectively. It had been

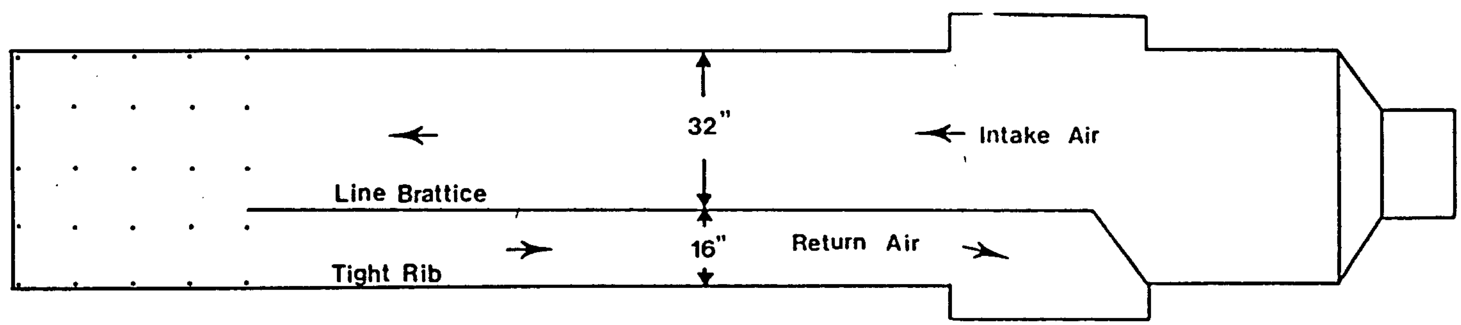

Fig. 4.1. Line Brattice Position in the Duct System

generally agreed, in order for the brattice to be effective in dust dilution, that the distance between the face and the end of line brattice should not be more than 20 ft.

4.2. Air Quantities

Four different air quantities were studied at each brattice distance. These air quantities were selected so that the dynamic similitude would be maintained. To maintain dynamic similitude, the Reynolds number for these flows were kept in the range of 20,000 to 80,000. They were 3400, 2400, 1800, and 1000 cfm, corresponding to full scale quantities of 17,000, 12,000, 9,000, and 5,000 cfm, respectively.

The various air quantities were obtained by controlling the intake area of the centrifugal fan. A stationary manometer was used to measure the velocity head at the intake duct, from which the air velocity could be derived. The intake air quantities were obtained by multiplying the cross section of the intake area and the air velocity. The air quantities employed in the tests would keep the Reynolds number in the range of turbulent flow and they were low enough to be considered as incompressible air.

4.3. Air Velocities

During the tests, it was observed that change of any combination of air quantity and brattice location would cause different rate of change of air velocity across the working area. Therefore, air velocity at each grid point was measured under different combination of brattice location, air quantity and with or without mining machines. The air velocity tended to be fluctuating, hence five measurements were taken at each grid point. The average air velocity was used as the air velocity throughout this study.

4.4. Methane Tests

Methane was first used to study the dust dispersion under sixteen combinations of air quantities and brattice distances. The tests were carried out without the presence of face machines in the beginning. After the completion of all the tests, the same procedures were repeated with the face machines present. These machines consisted of the continuous miner and shuttle car models. The layout for the test with the face machines is shown in Figure 4.2. The earlier setup was the same except for the face machine models.

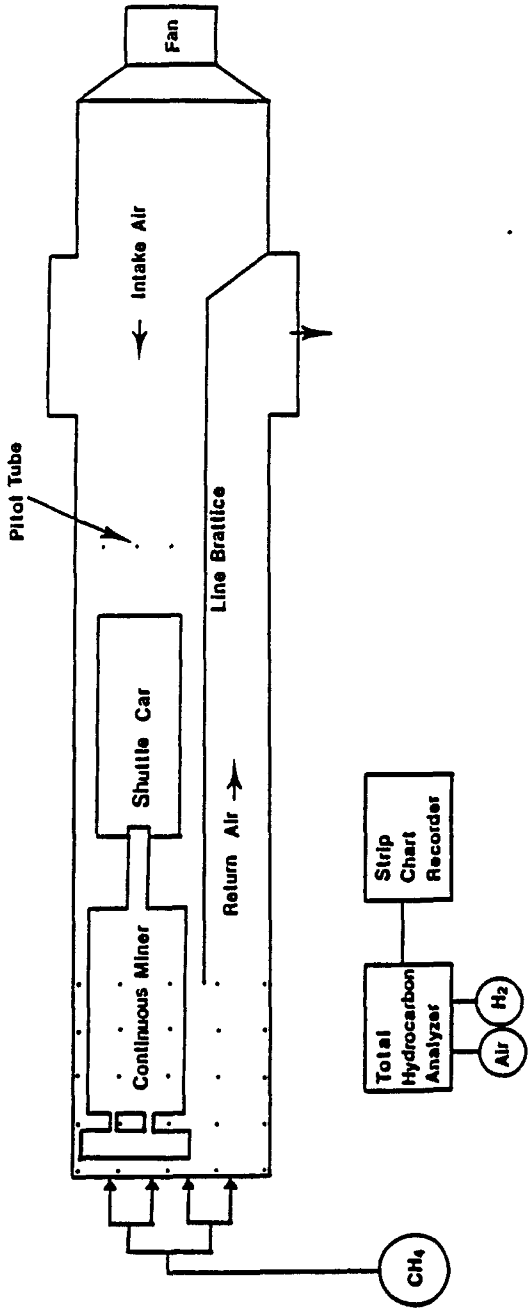

Fig. 4.2. Layout of Test With Face Machines Using Methane

During the test, methane was injected into the dead end of the duct system from a pressurized cylinder. The methane flowrate was set in order to be detectable by the Hydrocarbon Analyzer. It was chosen arbitrarily but was kept constant throughout all tests. The dust dispersion for a given air quantity and brattice distance was evaluated by measuring methane concentrations at each grid point. The concentrations were determined by averaging the readings from the Hydrocarbon Analyzer over a period of two minutes. There was a one minute interval between two consecutive readings so the instrument would yield a stable reading.

The readings were taken at a height of 12 inches above the bottom of the duct. This was equivalent to a full scale height of five feet. Overall, a one minute methane reading taken with the Hydrocarbon Analyzer was reproducible to about $\pm$30%. The test procedure is summarized as follows:

Step 1. Set brattice at desirable location; check and seal any apparent leakage.

Step 2. Turn on the Total Hydrocarbon Analyzer with the settings described in Chapter 3. Let the machine run for five minutes. This ensures no leftover hydrocarbon substance from the previous test.

Step 3. Adjust the manometer reading to zero.

Step 4. Turn on the face machines. This step is skipped in the tests when no face machines are present.

Step 5. Turn on the fan and adjust the intake area until the desirable reading is obtained with a manometer.

Step 6. Insert the copper tube into the duct through the hole at the starting grid point. Then turn on the strip chart recorder and adjust the reading to zero.

Step 7. Turn on the methane cylinder and adjust the flowmeter to obtain the preset flow rate.

Step 8. Wait for one minute before taking reading. Move the tubing to next measuring point after taking two minute reading. Repeat this step for all grid points.

Step 9. Turn off the methane cylinder.

Step 10. Turn off the strip chart recorder.

Step 11. Turn off the face machines. Skip this step if no face machine is present.

Step 12. Turn off the fan.

Step 13. Let the Hydrocarbon Analyzer run another five minutes before turning it off.

Step 14. Calculate the average methane concentration at each grid point.

4.5. Arizona Road Dust Test

Arizona Road Dust was utilized as a coal dust simulator after the methane tests were completed. It was used in the same sixteen combinations of brattice distance and air quantity. The tests were conducted with and without the presence of face machines. The complete layout of the test was the same as those setup in Figure 4.2 except that the dust feeder replaced the methane cylinder and the Ram-1 replaced the Analyzer.

In these tests, a Mark IX powder feeding machine was used to inject Road Dust into the dead end of the duct system. The dust feeding rate was fixed at 50 rpm screw speed throughout the tests. The dust concentration at any particular air quantity and brattice distance was measured by a Real-time Aerosol Monitor. Similar to the methane tests, the Road Dust concentration at each grid point was obtained by averaging the readings over a two minute period. There was a one minute interval between any two consecutive readings. The sampling was taken at a height of one foot above the bottom of the duct. The voltage output of the reading was connected to the Linear strip chart recorder. The dust readings obtained with the RAM-1 were generally reproducible to about ±40%. The procedure for road dust tests is summarized as follows:

Step 1. Set brattice at a desirable location. Check and seal any leakage throughout the duct system.

Step 2. Turn on the aerosol monitor and let it run for five minutes.

Step 3. Adjust the manometer reading to zero.

Step 4. Turn on the face machines. This step is skipped in the tests without the face machines.

Step 5. Turn on the fan and adjust the intake area until desirable air velocity is obtained.

Step 6. Insert the tubing into the duct through a hole to start measuring a grid point concentration. Turn on the strip chart recorder and adjust the output.

Step 7. Turn on the dust feeding machine.

Step 8. Wait for one minute before taking the grid point measurement. Take a two minute reading and then move the tubing to the next measuring point. Repeat this step for all grid points.

Step 9. Turn off the dust feeding machine.

Step 10. Turn off the strip chart recorder.

Step 11. Turn off the face machines. Skip this step if no face machines are present.

Step 12. Turn off the fan.

Step 13. Turn off the aerosol monitor.

Step 14. Calculate the average dust concentration at each grid point.

Chapter 5

Results and Discussion

5.1. General

The data collected from the tests without mining machines showed that the overall concentration (for both methane and Arizona Road Dust) in the face area decreased as the air quantity was increased at a specific brattice location. They also indicated that the extension of the line brattice toward the face would decrease the overall concentration of the dust simulating substances under the same air quantity. Although the concentration at most grid points dropped as the air quantity was increased, the rate of change of concentration varied from point to point. With the same air quantity, extending line brattice toward the face would decrease the overall concentration and the higher concentration area. The changes in concentration at each grid point caused by the extension of line brattice were much more uneven than those caused by increasing air quantity.

Similar trends were observed when the mining machines were present. However, a change of air quantity did not have as much effect when the line brattice was close to the face. The presence of mining machines caused the higher concentration area to occur in the area adjacent to the return airway. Also observed was the trapping of dust simulators around the open area with the presence of mining machines. In general, methane appeared to diffuse further and more evenly throughout the area than the road dust. However, the trend of concentration reduction responded to the changes in ventilation parameters remained close for methane and road dust.

5.2. Air Velocity

The air velocity data collected in the tests showed that the changes in air quantity and extension of line brattice resulted in a different rate of change for air velocity at each grid point. In general, the changes in air quantity caused more consistent changes in air velocity, while the extension of line brattice resulted in more radical changes in air velocity. However, some trends could be drawn by dividing the grid points into different zones.

For grid points which were adjacent to the wall of intake airway (points 1, 2, 3, 4 and 5), the increase of air quantity caused relatively consistent rate of increased for air velocity under same brattice location. With the same air quantity, the change of line brattice location caused uneven change of air velocity. Though the extension of line brattice a had large effect on the air velocity components parallel to the airway, little effect was observed on the air velocity components perpendicular to the airway. For the velocity components parallel to the airway, the rate of change could be summarized into three stages according to the locations of the grid points and the end of line brattice. In the first stage, where the end of line brattice was not extended beyond the grid points, the rate of change of air velocity component caused by extending line brattice one foot toward the face was under 50%. The largest increase rate in the air velocity occurred in the second stage where the end of brattice was extended one foot beyond the grid points. The rate of increase in the air velocity component ranged from 220% to 520%. In the final stage where the line brattice was extended further toward the face, the rate remained under 30%. Except for grid point 5, the velocity components parallel to the airway were much larger than those perpendicular to the airway.

For the grid points which were in the middle of intake airway (points 6, 7, 8, 9 and 10), similar trends could be observed. However, the largest rate of increase for air velocity occurred in the case where the line brattice was extended to one foot behind the grid points. The rate ranged from 280% to 480%. The rate or increase for air velocity decreased as the line brattice was extended further beyond the grid point; it became negative when the line brattice was extended from two feet to three feet beyond the grid points.

For grid points which were close to the line brattice in the intake airway (points 11, 12, 13, 14 and 15), patterns different from the previous two zones were observed. Both air velocity components increased as the end of line brattice was extended toward the grid points. However, the parallel components were much smaller than the perpendicular components. The parallel components became greater when the distance between face and end of the brattice was the same as that between face and grid point. At this particular line brattice position and a constant air quantity, the parallel components reached the highest magnitudes for the grid points. Both air velocity components started to drop as the line brattice was extended further toward the face.

For grid points which were close to the line brattice in the return airway (grid points 16, 17, 18, 19 and 20), both air quantity increase and extension of line brattice would increase both velocity components. The parallel components became greater than the perpendicular components when the end of line brattice was moved equal or beyond the grid points. In this area, the rate of air velocity change due to the change of air quantity was consistent. With a constant air quantity, the largest velocity change occurred when the end of line brattice was extended from one foot behind the grid point to the same location of the grid points.

For grid points which were adjacent to the wall of the return airway (grid points 21, 22, 23, 24 and 25), the extension of line brattice would decrease the perpendicular components and increase the parallel components. The air velocity became extremely high when the brattice was extended beyond the grid points. Also, larger rate of change occurred when the line brattice was moved from two feet to one foot behind the grid points. As in other zones, the change of air quantity resulted in the consistent change of air velocity components.

5.3. Isopachs and Low Concentration Zone

By observing the concentration data, it appeared that the effects of ventilation parameters on the reduction of dust concentration differed from grid point to grid point. Therefore in order to better understand the relationships among the location, air quantity, brattice distance, and dust concentration, it was necessary to study the dust dispersion behavior throughout the face.

To analyze the dust dispersion behavior across the face, data collected during the study were used to plot the substance isopachs through Surface II (Terrasciences Inc., 1986). To better visualize the changes in dust distribution, a low concentration zone was defined in every isopach. Since methane and road dust were measured differently and the presence of mining machines tended to increase the air pressure and change the flow pattern, the different values, listed in Table 5.1, were used to define a low concentration zone for each of those cases.

Both an extension of the line brattice and an increase of air quantity contributed to the increase in the area of a low concentration zone. The particular dimension of the low concentration zone was dependent on the air quantity and brattice distance; Figure 5.1 illustrates the general shape. The shape and trend of the low concentration zone were also affected by the presence of mining machines. In the tests without mining machines, the low concentration zone was found to be more prominent on the tight side of the duct.

The foremost point of its boundary was generally near to the end of the line brattice. When the mining machines were present, the low concentration zone appeared to be on the intake side of the duct and its boundary tended to be further toward the dead end. However, it should be pointed out that different values were used to define the low concentration zone.

Table 5.1. Upper Limit Values for Low Concentration Zone

	Methane, ppm	Road Dust, mg/m^3
With Machines	100	1.5
Without Machines	250	5.0

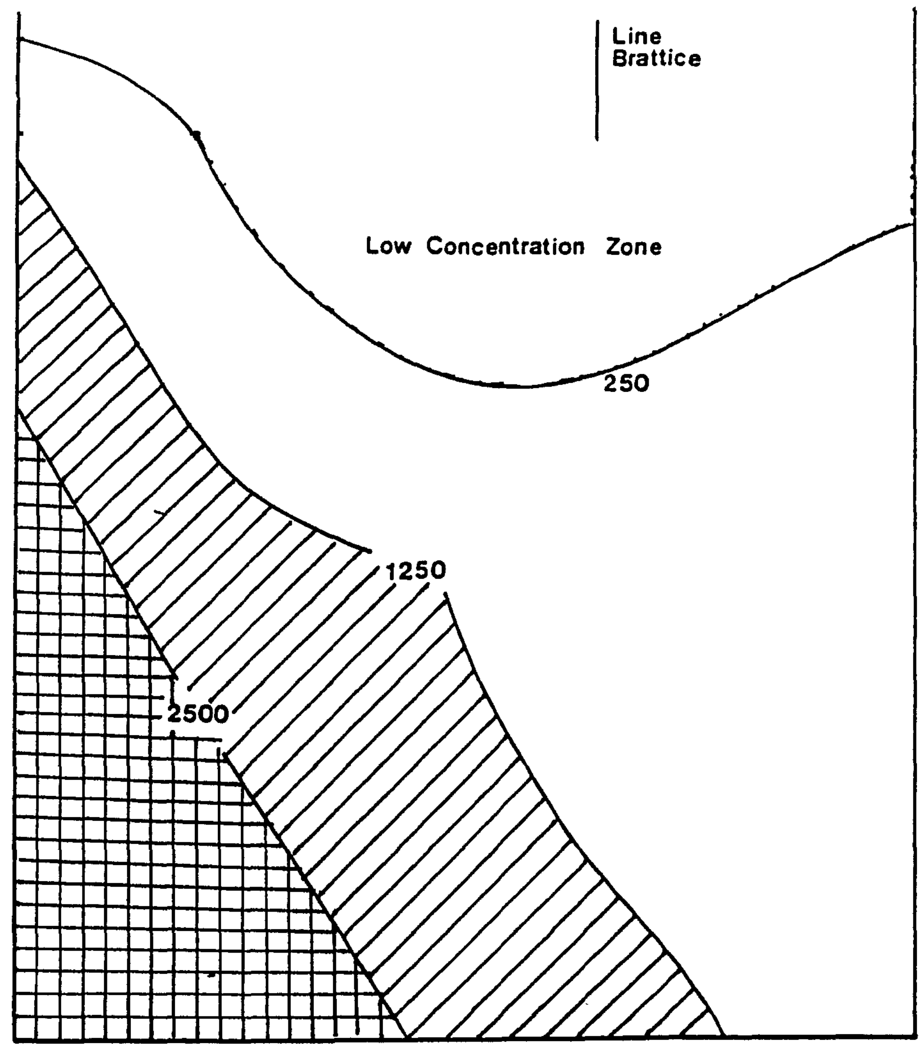

Fig. 5.1. Illustration of Low Concentration Zone (in ppm)

5.4. Increased Air Quantity

As stated earlier, the increase of air quantity reduces the overall face concentration of the dust simulating substances. The effect of the changes of air quantity on the overall reduction of dust concentration across the face area can be seen from Tables 5.2 and 5.3. Each specifies the change in air quantity that was tested at the four brattice distances. The percentages in these two tables were obtained by averaging the concentration changes of the four distances. The overall reduction trends were the same for both the methane and road dust experiments when the mining machines were not present. The smallest change in the air quantity resulted in the largest decrease in concentration.

The effectiveness of reducing concentrations through increased air quantity appeared to depend on the range of the air quantity. However, in those tests with mining machines, no similar overall reduction trends were found between the methane and the road dust. Though the smallest change in air quantity still resulted in the largest decrease in concentration for methane, different rates of changes were observed for those tests with road dust. This could be caused by the irregular feeding rate of the dust since the dust feeding machine tended to clog during the tests with the mining machines.

Table 5.2. Effects of the Air Quantity Change on Overall Substance Concentration Without Mining Machines

Increase in Air Quantity, cfm From	To	Changes of Concentration in Methane Tests	Road Dust Tests
1000	1800	-23%	-27%
1800	2400	-36%	-40%
2400	3400	-21%	-23%

Table 5.3. Effects of the Air Quantity Change on Overall Substance Concentration With Mining Machines

Increase in Air Quantity, cfm From	To	Changes of Concentration in Methane Tests	Road Dust Tests
1000	1800	-32%	-32%
1800	2400	-42%	-15%
2400	3400	- 7%	-41%

Increasing the air quantity not only reduced the overall concentration but also changed the shape of the low concentration zone. While the zone might be slightly deeper toward the face, the main effect of the increased air quantity was to widen the zone across the face area.

5.5. Brattice Distance Extensions

When the end of the brattice was extended toward the face, the overall face concentrations of the dust simulation substance decreased. Tables 5.4 and 5.5 show the effect that the specified brattice changes had on methane and road dust concentration without and with the mining machines, respectively. Since each specified brattice change was tested on all four air quantities, the percentages in these two tables were obtained by averaging the concentration changes of the four air quantities.

The line brattice extensions mainly deepened the low concentration zone toward the face. It also produced some widening of the zone. No similar trends of increasing rate of low concentration area were observed between methane and dust. The rate of change remained relatively the same for each substance regardless of the presence of mining machines. The extension of

Table 5.4. Effects of the Brattice Change on Overall Substance Concentration Without Mining Machines

Extension of Line Brattice, ft		Changes of Concentration in	
From	To	Methane Tests	Road Dust Tests
4	3	-22%	-21%
3	2	-24%	-27%
2	1	-19%	-31%

Table 5.5. Effects of the Brattice Change on Overall Substance Concentration With Mining Machines

Extension of Line Brattice, ft		Changes of Concentration in	
From	To	Methane Tests	Road Dust Tests
4	3	-58%	-24%
3	2	- 5%	-64%
2	1	-22%	-45%

the line brattice was less effective in decreasing the dust concentration when it was close to the face. The overall increase of low dust concentration area, when the line brattice was moved from two feet to one foot, was five percent with mining machines and none without mining machines. With the same air quantity, one eighth of the cases showed a decrease of low concentration area when the line brattice was moved one foot closer to the face.

5.6. Line Brattice and Air Quantity

Reductions in substance concentration caused by the combined effect of increasing the air quantity by 600 to 1000 cfm and extending the brattice by 1 foot are listed in Tables 5.6 to 5.9. The combined effect results in 55% and 49% average overall reduction of dust concentration for the tests with or without mine machines, respectively. The methane concentration reductions with and without mine machines were 50% and 52%, respectively. In the dust tests, when mine machines were not present, the average combined effects for any specific change of brattice or air quantity were close except for the change of air quantity from 2400 cfm to 3400 cfm.

Table 5.6. Combined Effect on Dust Concentration Reduction With Mining Machines

Extension of Line Brattice, ft	Increase in Air Quantity, cfm			Average
	1000-1800	1800-2400	2400-3400	
4-3	-53%	-65%	-67%	-62%
3-2	-80%	-43%	-66%	-63%
2-1	-39%	-45%	-37%	-40%
Average	-57%	-51%	-57%	-55%

Table 5.7. Combined Effect on Dust Concentration Reduction Without Mining Machines

Extension of Line Brattice, ft	Increase in Air Quantity, cfm			Average
	1000-1800	1800-2400	2400-3400	
4-3	-57%	-63%	-33%	-51%
3-2	-39%	-56%	-55%	-50%
2-1	-53%	-51%	-33%	-46%
Average	-50%	-57%	-40%	-49%

Table 5.8. Combined Effects on Methane Concentration Reduction With Mining Machines

Extension of Line Brattice, ft	Increase in Air Quantity, cfm			Average
	1000-1800	1800-2400	2400-3400	
4-3	-72%	-68%	-49%	-63%
3-2	-33%	-29%	-17%	-26%
2-1	-54%	-73%	-55%	-61%
Average	-53%	-57%	-40%	-50%

Table 5.9. Combined Effect of Methane Concentration Reduction Without Mining Machines

Extension of Line Brattice, ft	Increase in Air Quantity, cfm			Average
	1000-1800	1800-2400	2400-3400	
4-3	-60%	-58%	-61%	-60%
3-2	- 9%	-47%	-29%	-28%
2-1	-62%	-76%	-63%	-67%
Average	-44%	-60%	-51%	-52%

However, when the mine machines were present, the combined effect due to the change of moving the line brattice from two feet to one foot away from the face was less significant. With methane as the dust simulator, moving the line brattice from 3 feet to 2 feet away from the face resulted in the least average reduction in concentration.

5.7. Others

Air Quantity vs. Brattice Distance. Both increasing air quantity and extending line brattice toward the face would decrease the overall dust concentration effectively. In the tests with mining machines, extending the line brattice toward the face resulted in a greater reduction of dust concentration. Even with low air quantity, most of the grid points were within the low concentration zone. When the line brattice was set at less than two feet from the face, the change of air quantity did not have much effect on the area of low concentration zone.

In those tests with Road Dust, when the line brattice was set at one foot away from the face, the area of the low concentration zone was reduced and overall dust concentration increased as the air quantity was increased. But, in those tests without mining machines, the magnitude of the reduction of overall concentration was significant when the line brattice was set close to the face.

Methane vs. Road Dust. The effects of ventilation parameters on the change of methane and road dust concentrations compared well without the presence of machines. The presence of machines, resulted in more irregular high dust concentration points. Overall, except for the cases where mining machines were present and the line brattice was one foot from the face, the same trends were evident between both dust simulators. However, the methane tended to diffuse more evenly and, perhaps, a little farther from the injection points.

Face Machines vs. No Face Machines. The presence of mine machines changed the flow pattern across the face area. It resulted in the shifting of high concentration points and a change in the shape of the low concentration zone. The overall concentration reductions caused by the presence of mining machines were about 70% and 80% for dust and methane, respectively. The high concentration points were pushed toward the area in front of the return airway when face machines were present; the low concentration zone was more prominent around the intake area. Also the drum rotation tends to increase the concentration around the intake area at the end of the line brattice.

Area of Low Concentration Zone. Tables 5.10 to 5.13 list the number of grid points within the low concentration zone under different combinations of air quantity and brattice location. The number of grid points roughly reflect the area of low concentration zone. Except for the tests of road dust with mining machines, increasing air quantity from 1800 cfm to 2400 cfm resulted in the largest increase of overall low concentration area; and increasing air quantity resulted in minimal effect after air quantity reaches 2400 cfm.

When methane was used as dust simulator, for a constant air quantity, minimum effects occurred when line brattice was extended from 3 ft toward 2 ft away from face. While in the Road Dust tests, minimum effects occurred when the line brattice was extended from 2 ft toward 1 ft away from the face.

The combined effect on the low concentration zone was a widening and deepening of its dimensions. Except for two cases in the dust tests with mine machines, no increase in the number of grid points in the low concentration zone was observed. Table 5.14 lists the total increase of grid points in each different setup. The largest increase in the number of grid points occurred with the methane tests and with mine machines. The combined effect on the increase of low concentration area is about the same on the other setup.

Table 5.10. Number of Grid Points Within Low Methane Concentration Zone With Mining Machines

Line Brattice Location, ft	Air Quantity, cfm				Total
	1000	1800	2400	3400	
4	4	6	11	11	32
3	7	13	15	19	54
2	7	10	18	16	51
1	18	19	21	22	80
Total	36	48	65	68	

Table 5.11. Number of Grid Points Within Low Methane Concentration Zone Without Mining Machines

Line Brattice Location, ft	Air Quantity, cfm				Total
	1000	1800	2400	3400	
4	3	5	5	6	19
3	8	8	10	11	37
2	9	8	15	16	48
1	12	18	20	20	70
Total	32	39	50	53	

Table 5.12. Number of Grid Points Within Low Dust Concentration Zone With Mining Machines

Line Brattice Location, ft	Air Quantity, cfm 1000	1800	2400	3400	Total
4	10	11	17	16	54
3	10	15	17	18	60
2	14	23	21	22	80
1	23	22	20	19	84
Total	57	71	75	75	

Table 5.13. Number of Grid Points Within Low Dust Concentration Zone Without Mining Machines

Line Brattice Location, ft	Air Quantity 1000	1800	2400	3400	Total
4	4	3	7	10	24
3	8	8	14	11	41
2	12	16	17	18	63
1	12	12	19	20	63
Total	36	39	57	59	

Table 5.14. Combined Effects on Overall Increase of Number of Grid Points Within Low Concentration Zone

	Dust	Methane
With Machines	39	62
Without Machines	46	49

CHAPTER 6

ANALYSIS OF DUST CONCENTRATION

In order to study the effect of ventilation parameters on dust concentration in the working area, with or without the presence of face machines, the data obtained from the tests were analyzed to examine the correlation between the concentration and the parameters.

Data obtained from the tests show that the rate of change of dust concentration differs from point to point. Therefore, the analysis starts with examining the correlation existing between the dust concentration and ventilation parameters at each grid point. In the process, both road dust and methane concentrations at each grid point, with or without mining machines, are treated as dependent variables, whereas the ventilation parameters are considered as the independent variables. Procedure CORR in SAS (SAS Institute Inc., 1985a) is first used to examine the correlation existing between the concentration and the ventilation parameters as well as that between the methane concentration and road dust concentration. Then the multiple regression procedure STEPWISE is used to obtain the statistical model between the dust concentration and ventilation parameters.

6.1. Analysis of Dust Concentration at Grid Point

The CORR procedure (SAS Institute Inc., 1985b) computes correlation coefficients between variables. Correlation measures the closeness of a linear relationship between two variables. If one variable X can be expressed exactly as a linear function of another variable Y, then the correlation is 1 or -1, depending on whether the two variables are directly related or inversely related. A correlation of zero between two variables means that each variable has no linear predictive ability for the other. If the values are normally distributed, then a correlation of zero means that the variables are independent of one another. The sample correlation estimating the true correlation is calculated here. It is:

$$R_{XY} = \Sigma(X-\overline{X}) \times \Sigma(Y-\overline{Y})/(\Sigma(X-\overline{X})^2 \times \Sigma(Y-\overline{Y})^2)^{1/2}$$

Where $\overline{X}$ and $\overline{Y}$ are the sample mean of X and Y.

The correlation coefficients between the concentrations of the dust simulators and the line brattice distances at each grid point, with or without face machines, are shown in Figures 6.1 to 6.4. The number of observations for each grid point is 16 , and the significance probability of the correlation for each grid

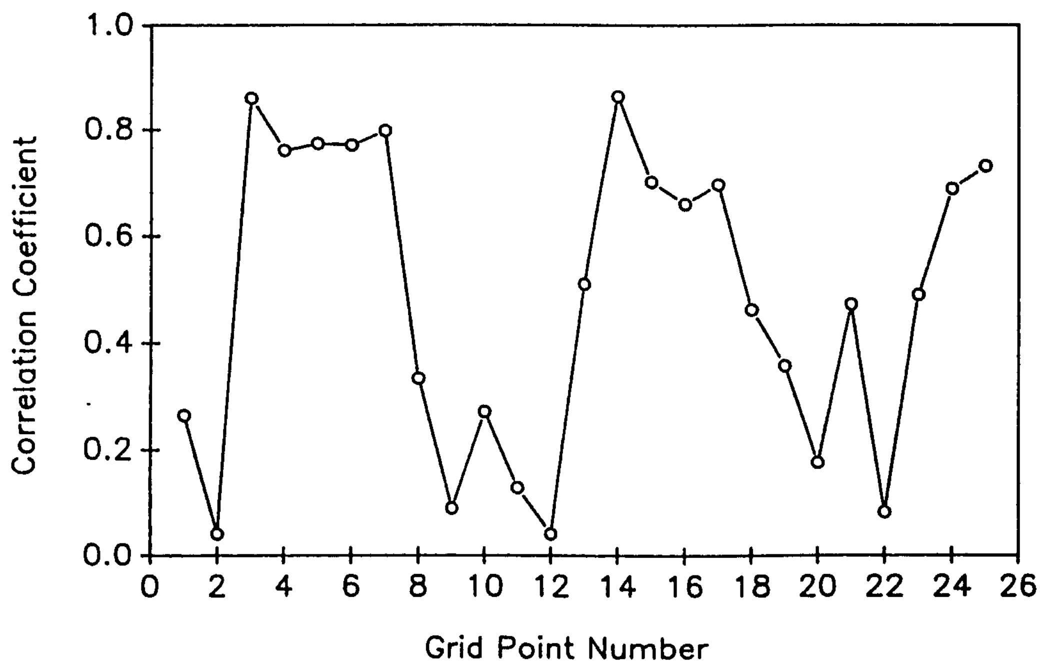

Significance probability of correlation

1	0.3233	6	0.0005	11	0.6365	16	0.0055	21	0.0647
2	0.8788	7	0.0002	12	0.8804	17	0.0027	22	0.7632
3	0.0001	8	0.2075	13	0.0437	18	0.0714	23	0.0539
4	0.0006	9	0.7417	14	0.0001	19	0.1741	24	0.0032
5	0.0004	10	0.3092	15	0.0025	20	0.5150	25	0.0013

Fig. 6.1. Correlation Coefficients Between Line Brattice Distance and Methane Concentration With Face Machines

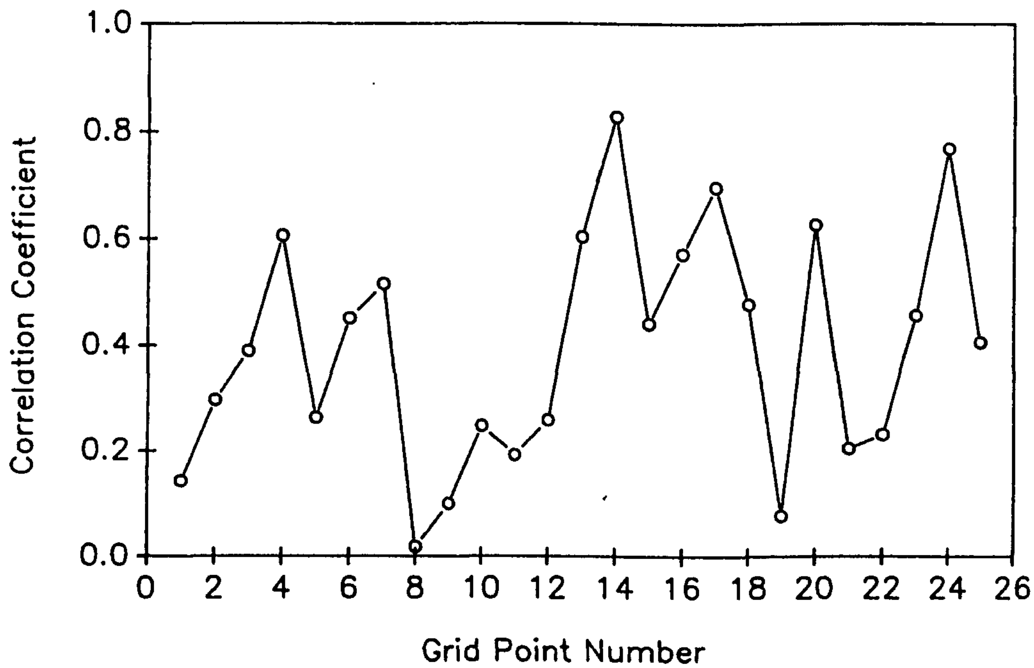

Significance probability of correlation

1	0.6000	6	0.0795	11	0.4755	16	0.0208	21	0.4403
2	0.2653	7	0.0412	12	0.3349	17	0.0028	22	0.3886
3	0.1368	8	0.9466	13	0.0135	18	0.0618	23	0.0761
4	0.0129	9	0.7161	14	0.0001	19	0.7783	24	0.0005
5	0.3252	10	0.3558	15	0.0875	20	0.0096	25	0.1186

Fig. 6.2. Correlation Coefficients Between Line Brattice and Road Dust Concentration With Face Machines

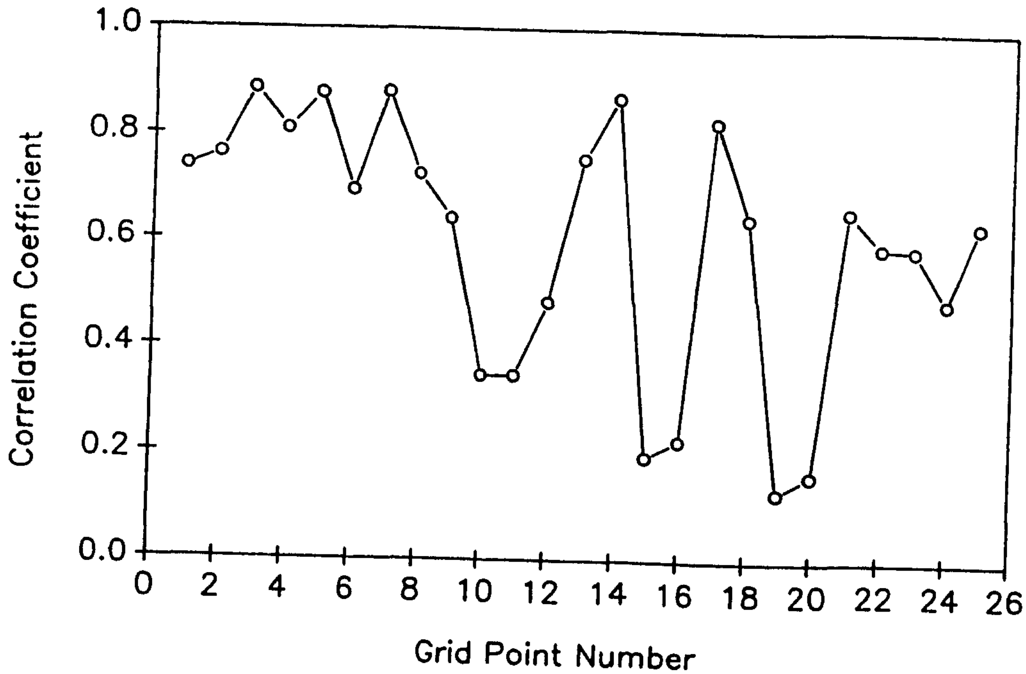

Significance probability of correlation

1	0.0011	6	0.0029	11	0.1887	16	0.4002	21	0.0055
2	0.0006	7	0.0001	12	0.0573	17	0.0001	22	0.0160
3	0.0001	8	0.0015	13	0.0007	18	0.0068	23	0.0168
4	0.0001	9	0.0075	14	0.0001	19	0.6305	24	0.0554
5	0.0001	10	0.1887	15	0.4684	20	0.5479	25	0.0084

Fig. 6.3. Correlation Coefficients Between Line Brattice Distance and Methane Concentration Without Face Machines

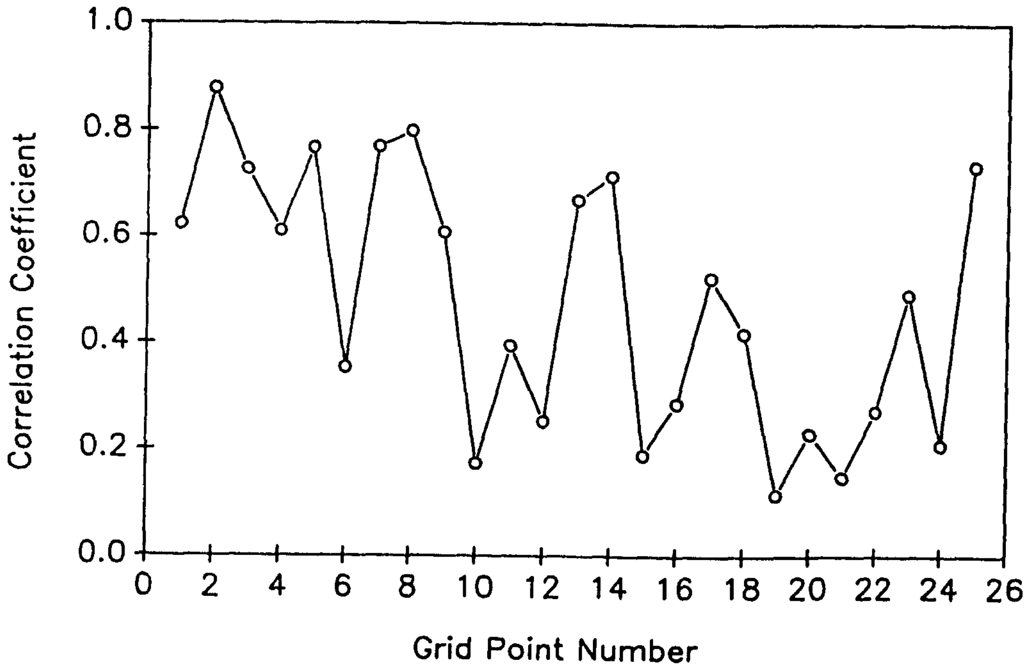

Significance probability of correlation

1	0.3233	6	0.0005	11	0.6365	16	0.0055	21	0.0647
2	0.8788	7	0.0002	12	0.8804	17	0.0027	22	0.7632
3	0.0001	8	0.2075	13	0.0437	18	0.0714	23	0.0539
4	0.0006	9	0.7417	14	0.0001	19	0.1741	24	0.0032
5	0.0004	10	0.3092	15	0.0025	20	0.5150	25	0.0013

Fig. 6.4. Correlation Coefficients Between Line Brattice and Road Dust Concentration Without Face Machines

point is listed in the figures. Without face machines present, higher linear correlation exists at the area in front of the intake airway. However, lower linear correlations are observed for grid points 10 and 11, which are located far away from the face. With face machines present, the correlation coefficients are lower than those without machines, especially for those grid points located far away from the face.

For different line brattice distance, one set of correlation coefficients between concentrations of dust simulators and air quantity at each grid points were calculated. The correlation coefficients and the significance probabilities of the correlations are shown in Figures 6.5 to 6.8. The number of observations for each grid point is 4 at each brattice distance. In general, the coefficients are lower than those for line brattice distance. However, higher linear correlation exists in the area adjacent to the return airway. Also, the correlation becomes higher as the brattice distance increases.

The correlation coefficients between the concentrations of methane and road dust at each grid point and the significance probabilities of the correlations, with or without face machines, are shown in Figures 6.9 and 6.10, respectively. The number of observations for each grid point is 16. Again, higher correlation coefficients are observed when

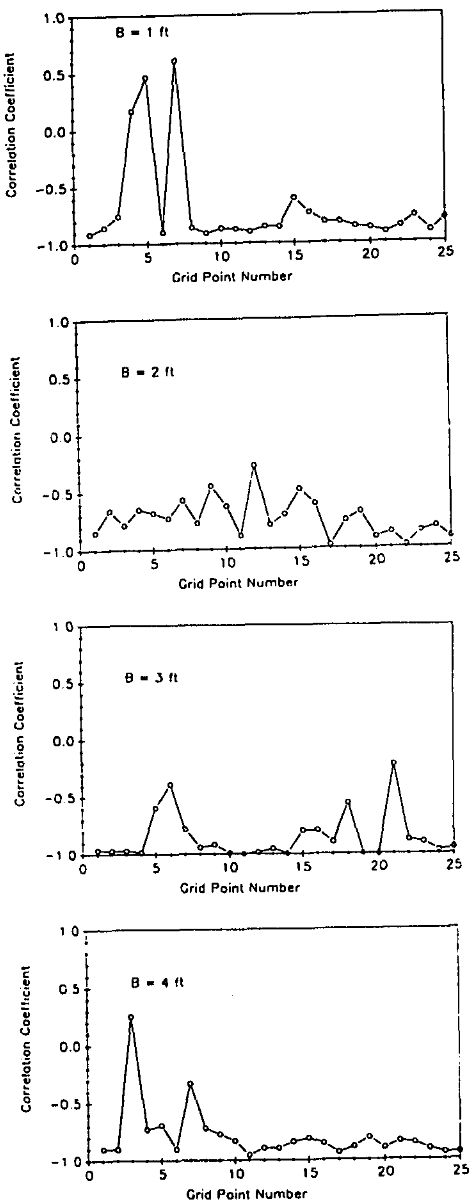

MW	VS Q B1	B2	B3	B4
1	0.0883	0.1533	0.0350	0.1004
2	0.1439	0.3391	0.0279	0.0970
3	0.2421	0.2138	0.0314	0.7485
4	0.8307	0.3494	0.0146	0.2686
5	0.5361	0.3164	0.4034	0.3039
6	0.0983	0.2699	0.6109	0.0981
7	0.3923	0.4254	0.2177	0.6666
8	0.1383	0.2274	0.0581	0.2780
9	0.0884	0.5492	0.0820	0.2253
10	0.1297	0.3730	0.0101	0.1676
11	0.1250	0.1146	0.0023	0.0437
12	0.0996	0.7227	0.0146	0.1042
13	0.1439	0.2078	0.0463	0.1030
14	0.1403	0.2984	0.0041	0.1592
15	0.3922	0.5151	0.2047	0.1868
16	0.2641	0.3861	0.2047	0.1445
17	0.1838	0.0242	0.1040	0.0643
18	0.1820	0.2408	0.4434	0.1132
19	0.1403	0.3145	0.0035	0.1916
20	0.1290	0.0940	0.0041	0.1007
21	0.0848	0.1337	0.7804	0.1592
22	0.1417	0.0212	0.1207	0.1444
23	0.2283	0.1438	0.1006	0.0909
24	0.0977	0.1822	0.0302	0.0602
25	0.2024	0.0851	0.0500	0.0585

Fig. 6.5. Correlation Coefficients Between Air Quantity and Methane Concentration With Face Machines

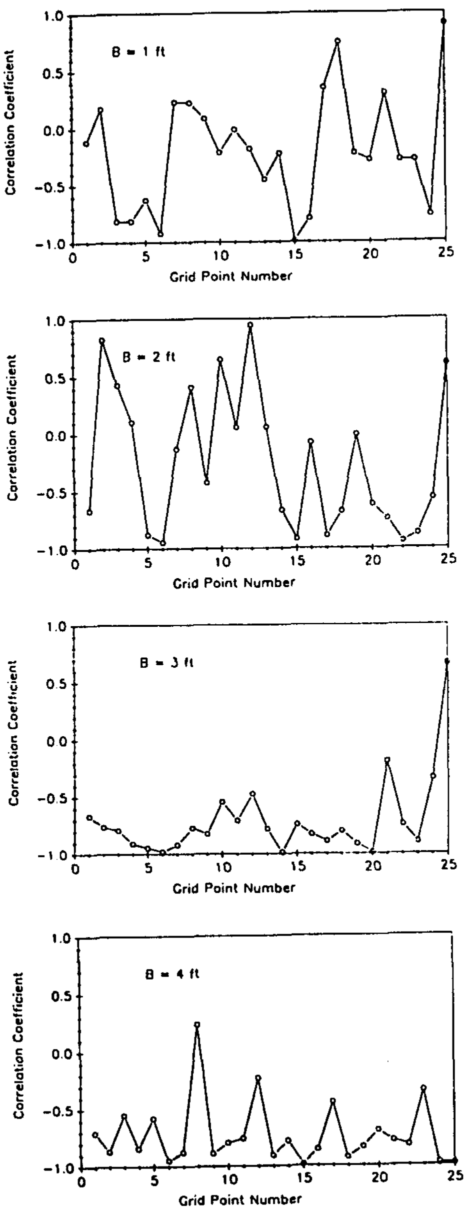

DW	VS Q B1	B2	B3	B4
1	0.8836	0.3342	0.1762	0.2945
2	0.8236	0.1762	0.2386	0.1344
3	0.1842	0.5714	0.2076	0.4490
4	0.1842	0.8953	0.0923	0.1571
5	0.3710	0.1211	0.0536	0.4199
6	0.0775	0.0540	0.0212	0.0502
7	0.7689	0.8692	0.0806	0.1216
8	0.7744	0.5918	0.2277	0.7621
9	0.9144	0.5760	0.1756	0.1115
10	0.7855	0.3539	0.4577	0.2055
11	0.9870	0.9429	0.2946	0.2421
12	0.8158	0.0546	0.5273	0.7693
13	0.5483	0.9429	0.2198	0.0917
14	0.7752	0.3336	0.0140	0.2180
15	0.0110	0.0840	0.2600	0.0159
16	0.2045	0.9238	0.1745	0.1439
17	0.6496	0.1105	0.1116	0.5571
18	0.2572	0.3229	0.2022	0.0739
19	0.7752	0.9904	0.0894	0.1634
20	0.7143	0.3817	0.0140	0.3049
21	0.6983	0.2580	0.8129	0.2180
22	0.7142	0.0602	0.2584	0.1795
23	0.7142	0.1272	0.1074	0.6562
24	0.2293	0.0461	0.6622	0.0231
25	0.0992	0.3982	0.3389	0.0154

Fig. 6.6. Correlation Coefficients Between Air Quantity and Road Dust Concentration With Face Machines

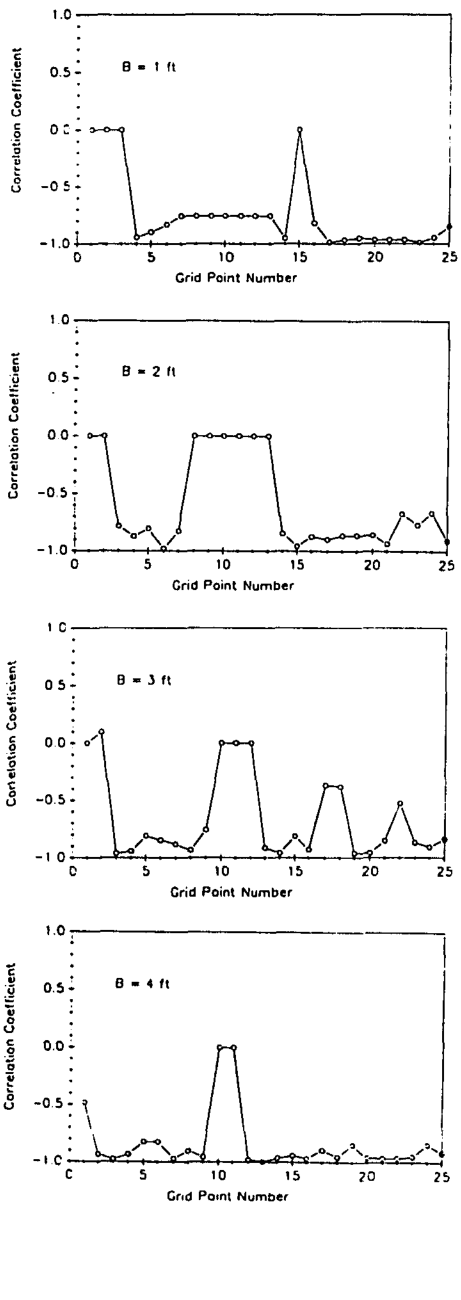

MN	VS Q B1	B2	B3	B4
1	1.0000	1.0000	0.7579	0.5167
2	1.	1.	0.9022	0.0662
3	1.	0.2174	0.0400	0.0235
4	0.0567	0.1283	0.0585	0.0671
5	0.1019	0.1967	0.1896	0.1748
6	0.1668	0.0196	0.1521	0.1754
7	0.2421	0.1737	0.1172	0.0282
8	0.2421	1.	0.0660	0.0968
9	0.2421	1.	0.2421	0.0440
10	0.2421	1.	1.	1.
11	0.2421	1.	1.	1.
12	0.2421	1.	1.	0.0197
13	0.2421	1.	0.0856	0.0055
14	0.0484	0.1546	0.0412	0.0367
15	1.	0.0435	0.1866	0.0581
16	0.1801	0.1284	0.0722	0.0347
17	0.0122	0.1029	0.6319	0.1050
18	0.0336	0.1360	0.6194	0.0462
19	0.0484	0.1391	0.0406	0.1532
20	0.0334	0.1434	0.0412	0.0419
21	0.0337	0.0653	0.1480	0.0367
22	0.0349	0.3278	0.4744	0.0378
23	0.0106	0.2317	0.1306	0.0497
24	0.0530	0.3349	0.0920	0.1538
25	0.1487	0.0945	0.1608	0.0838

Fig. 6.7. Correlation Coefficients Between Air Quantity
and Methane Concentration Without Face Machines

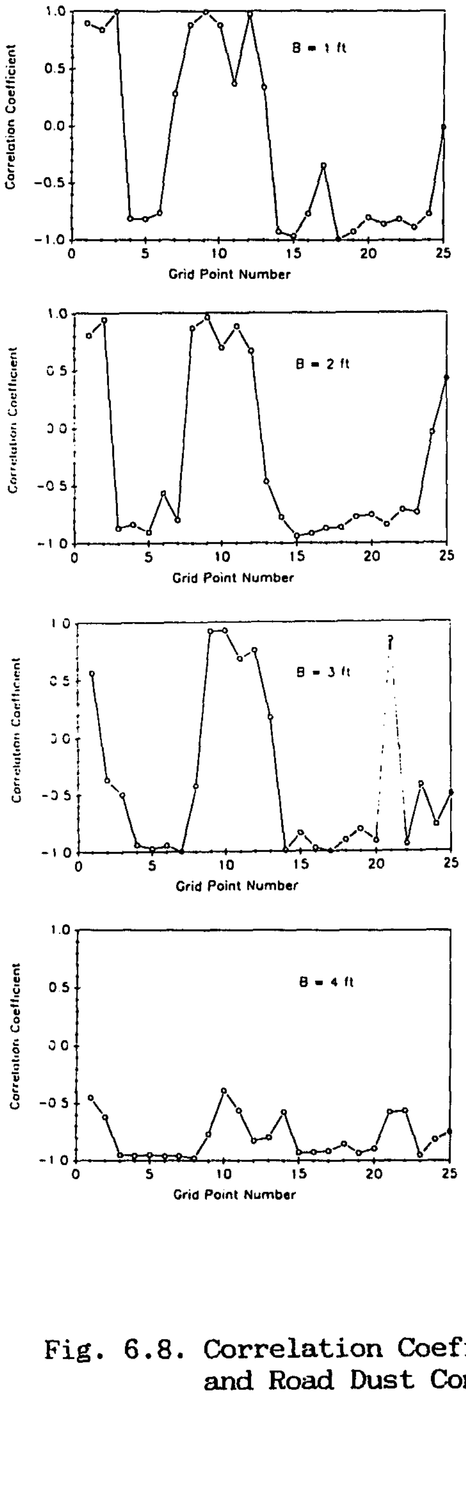

DN	VS Q B1	B2	B3	B4
1	0.1082	0.1953	0.4345	0.5490
2	0.1648	0.0570	0.6321	0.3792
3	0.0051	0.1307	0.5005	0.0506
4	0.1863	0.1635	0.0604	0.0426
5	0.1831	0.0961	0.0282	0.0511
6	0.2367	0.4337	0.0556	0.0419
7	0.7183	0.2005	0.0017	0.0406
8	0.1207	0.1326	0.5760	0.0197
9	0.0088	0.0392	0.0783	0.2311
10	0.1238	0.3051	0.0724	0.6113
11	0.6324	0.1167	0.3167	0.4367
12	0.0530	0.3339	0.2440	0.1736
13	0.6608	0.5311	0.8257	0.2016
14	0.0745	0.2256	0.0915	0.4238
15	0.0325	0.0591	0.1595	0.0708
16	0.2315	0.0837	0.0312	0.0745
17	0.6562	0.1294	0.0013	0.0847
18	0.0062	0.1335	0.0798	0.1452
19	0.0745	0.2273	0.1935	0.0669
20	0.1982	0.2460	0.0915	0.1067
21	0.1391	0.1584	0.1503	0.4238
22	0.1834	0.2879	0.0628	0.4354
23	0.1140	0.2648	0.5848	0.0499
24	0.2285	0.9559	0.2281	0.1851
25	0.9876	0.5759	0.4983	0.2489

Fig. 6.8. Correlation Coefficients Between Air Quantity and Road Dust Concentration Without Face Machines

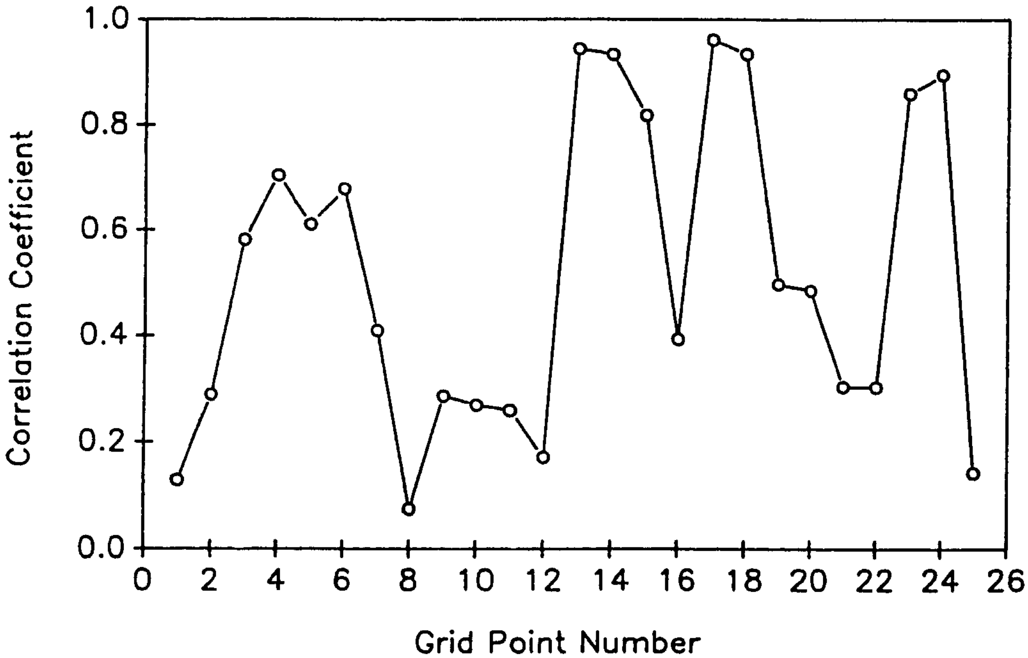

Significance probability of correlation

1	0.6371	6	0.0039	11	0.3320	16	0.1316	21	0.2515
2	0.2768	7	0.1155	12	0.5264	17	0.0001	22	0.2545
3	0.0405	8	0.7843	13	0.0001	18	0.0001	23	0.0001
4	0.0023	9	0.2831	14	0.0001	19	0.0504	24	0.0001
5	0.0121	10	0.3145	15	0.0001	20	0.0566	25	0.5999

Fig. 6.9. Correlation Coefficients Between Methane Concentration and Road Dust Concentration With Face Machines

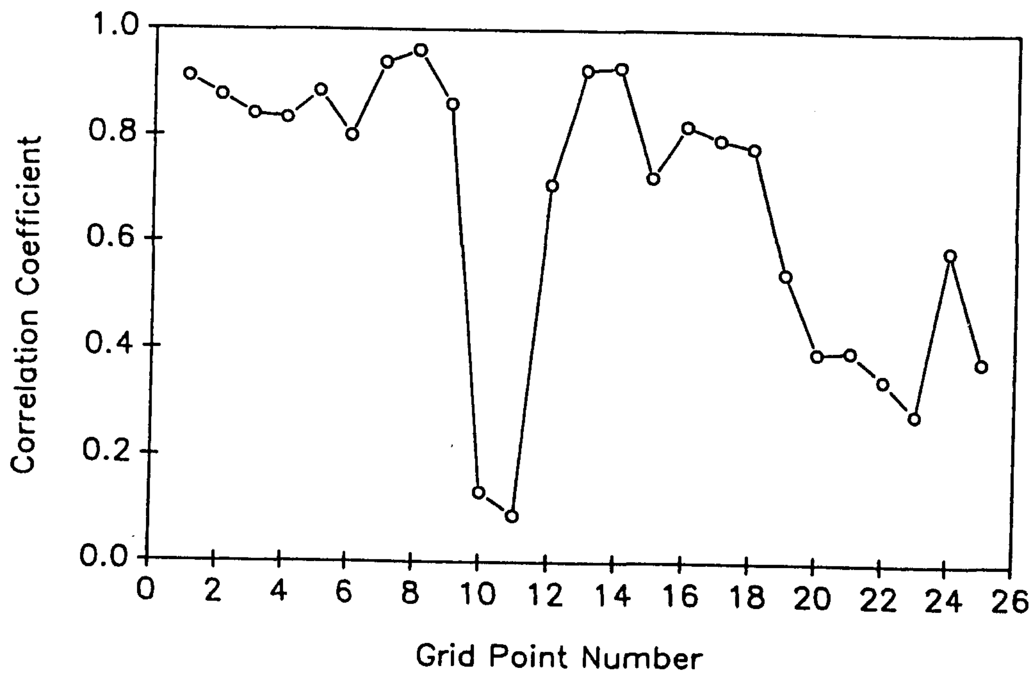

Significance probability of correlation

1	0.0001	6	0.0002	11	0.7446	16	0.0001	21	0.1258
2	0.0001	7	0.0001	12	0.0021	17	0.0002	22	0.1899
3	0.0001	8	0.0001	13	0.0001	18	0.0004	23	0.2891
4	0.0001	9	0.0001	14	0.0001	19	0.0295	24	0.0163
5	0.0001	10	0.6248	15	0.0015	20	0.1299	25	0.1451

Fig. 6.10. Correlation Coefficients Between Methane Concentration and Road Dust Concentration Without Face Machines

face machines are not present. Without face machines, high coefficients are observed except for the grid points located in the area close to the wall adjacent to the return airway. With face machines, the concentrations of those two dust simulators correlate well only at grid points close to the face, where the air velocities are relatively low.

6.2. Regression Model for Dust Concentration

Model Selection.

The independent and dependent variables selected in this study are specified as follows:

Independent Variables

X_1 is the air velocity at the grid point, with or without face machines (VN or VW), in 1000 fpm,

X_2 is the distance between the end of brattice and the grid point (DIS), in ft,

X_3 is the brattice distance (B), in ft,

X_4 is the relative distance between the grid point and the end of brattice in the x direction (DX), in ft, and

X_5 is the relative distance between the gird point and the end of brattice in the y-direction (DY), in ft.

Dependent Variables

Y_1 is the logarithm of methane concentration at the grid point without face machines (CMN), in ppm,

Y_2 is the logarithm of dust concentration at the grid point without face machines (CDN), in g/m^3,

Y_3 is the logarithm of methane concentration at the grid point with face machines (CMW), in ppm, and

Y_4 is the logarithm of dust concentration at the grid point with face machines (CDW), in g/m^3.

A full second order model was adopted to investigate the interacting effects of the different parameters. The initial model was as below:

$$Y = b_0 + \Sigma_{i=1}^{5} (b_i X_i + b_{ii} X_i) + \Sigma_{i=1}^{4} \Sigma_{j=i+1}^{5} b_{ij} X_i X_j$$

The model was reduced by using PROC STEPWISE (SAS Institute Inc., 1985c) to eliminate all the insignificant parameters at .15 level. The STEPWISE procedure provides five methods for stepwise regression. It is most helpful for exploratory analysis, because it gives insight into the relationships between the independent variables and the dependent variables. It is useful to find which variables should be included in a regression model.

The stepwise selection technique is used to select the models for all the four dependent variables. It begins with no variables in the model. For each of the independent variables, STEPWISE calculates F statistics reflecting the variable's contribution to the model if it is included. For a variable to be added, the F statistics must be significant at the SLENTRY = level, which is default as .15 in this study. After a variable is added , however, the stepwise method looks at all the variables already included in the model and deletes any variable that does not produce an F statistic significant at the SLSTAY = level, which is default as .15 in this study. Only after this check is made and the necessary deletions accomplished can another variable be added to the model. The stepwise process ends when none of the variables outside the model has an F statistic significant at the SLENTRY = level and every variable in the model is significant at the SLSTAY = level or when the variable to be added to the model is one just deleted from it. The statistical properties for each final model are listed in Table 6.1. The information indicates the model for methane concentration without face machines fits well. Models for methane with machines and dust without machines are fair, while the model for dust with machines fits poorly. The coefficients for the empirical models to predict the dust concentrations are listed in Table 6.2.

Table 6.1. Printout for Final Models

Y1

STEP 16 VARIABLE VNDX ENTERED R SQUARE = 0.83505708 C(P) = 14.17728099

	DF	SUM OF SQUARES	MEAN SQUARE	F	PROB>F
REGRESSION	12	1018.67263077	84.88938590	163.27	0.0001
ERROR	387	201.21119969	0.51992558		
TOTAL	399	1219.88383046			

	B VALUE	STD ERROR	TYPE II SS	F	PROB>F
INTERCEPT	4.82517173				
VN	-1.63145781	0.11548284	103.76668973	199.58	0.0001
DIS	1.69923851	0.17150927	51.03576884	98.16	0.0001
DX	-0.37496561	0.08932072	9.15774317	17.61	0.0001
DY	1.89486558	0.13925952	96.26052047	185.14	0.0001
DX2	-0.26003701	0.04179028	20.13089107	38.72	0.0001
DY2	-0.19966096	0.05435917	7.01425897	13.49	0.0003
VNDX	0.16742956	0.06032584	4.00496478	7.70	0.0058
VNDY	0.83167781	0.09342989	41.19834212	79.24	0.0001
DISB	-0.21038521	0.02695626	31.90659491	61.37	0.0001
DISDY	-0.26113611	0.04567313	16.99626159	32.69	0.0001
BDX	-0.11923562	0.03986169	4.65202239	8.95	0.0030
BDY	-0.19644606	0.02666303	99.46420193	191.30	0.0001

Y2

STEP 15 VARIABLE VNDY REMOVED R SQUARE = 0.70940047 C(P) = 14.60574247

	DF	SUM OF SQUARES	MEAN SQUARE	F	PROB>F
REGRESSION	13	567.53797267	43.65676714	72.48	0.0001
ERROR	386	232.48683171	0.60229749		
TOTAL	399	800.02480458			

	B VALUE	STD ERROR	TYPE II SS	F	PROB>F
INTERCEPT	3.19195945				
VN	-0.93498542	0.27671709	6.87620405	11.42	0.0008
DIS	0.45504308	0.07597528	21.60591331	35.87	0.0001
B	-1.41315149	0.25078246	19.13280136	31.77	0.0001
DX	-0.97080090	0.10543716	51.06037269	84.78	0.0001
DY	1.20349105	0.12675250	54.29798532	90.15	0.0001
VN2	0.15785960	0.05170204	5.61485842	9.32	0.0024
B2	0.22903791	0.04954271	12.87259930	21.37	0.0001
VNB	-0.11224902	0.07475394	1.35802568	2.25	0.1340
DISDX	0.10081360	0.02846831	7.55311344	12.54	0.0004
DISDY	-0.16424327	0.03576475	12.70210899	21.09	0.0001
BDX	0.12245004	0.04106713	5.35476254	8.89	0.0030
BDY	-0.19208201	0.03636746	16.78344079	27.87	0.0001
DXDY	0.07724990	0.02215909	7.31986208	12.15	0.0005

Y3

STEP 17 VARIABLE VNB ENTERED R SQUARE = 0.63643558 C(P) = 10.36819091

	DF	SUM OF SQUARES	MEAN SQUARE	F	PROB>F
REGRESSION	13	208.77179795	16.05936907	51.98	0.0001
ERROR	386	119.26108266	0.30896654		
TOTAL	399	328.03288061			

	B VALUE	STD ERROR	TYPE II SS	F	PROB>F
INTERCEPT	4.80381633				
VN	-0.87472551	0.21160184	5.27978416	17.09	0.0001
DIS	-0.76401524	0.10217056	17.27682400	55.92	0.0001
B	0.89617811	0.19599161	6.45989055	20.91	0.0001
DX	0.31425532	0.08695771	4.03515767	13.06	0.0003
VN2	0.09588032	0.04607883	1.33772717	4.33	0.0381
B2	-0.19627761	0.03543836	9.47777835	30.68	0.0001
VNB	-0.11621920	0.05700581	1.32876836	4.30	0.0388
VNDY	0.19519851	0.06353548	2.91629752	9.44	0.0023
DISB	0.28847761	0.04500929	12.69159952	41.08	0.0001
DISDX	0.11379844	0.02752169	5.23611565	16.95	0.0001
BDX	-0.13823060	0.03049706	6.34959958	20.55	0.0001
BDY	0.12040085	0.01907553	12.30884223	39.84	0.0001
DXDY	0.06597260	0.01930884	3.60683587	11.67	0.0007

Y4

STEP 6 VARIABLE B ENTERED R SQUARE = 0.55184203 C(P) = 11.79448450

	DF	SUM OF SQUARES	MEAN SQUARE	F	PROB>F
REGRESSION	6	287.13945636	47.85657606	80.65	0.0001
ERROR	393	233.18962862	0.59335783		
TOTAL	399	520.32908518			

	B VALUE	STD ERROR	TYPE II SS	F	PROB>F
INTERCEPT	0.46293720				
B	0.18659176	0.05627364	6.52366433	10.99	0.0010
DY	0.27055393	0.04640583	20.16876292	33.99	0.0001
VNB	-0.32554717	0.04053305	38.27595021	64.51	0.0001
VNDY	0.23157491	0.05981270	8.89432224	14.99	0.0001
BDX	-0.08977855	0.01193298	33.58644956	56.60	0.0001
DXDY	-0.07916923	0.01747779	12.17464550	20.52	0.0001

Table 6.2. Coefficients from Models Built for Dust Concentration

Coefficients	Y_1(CMN)	Y_2(CDN)	Y_3(CMW)	Y_4(CDW)
b_0	4.82517	3.19196	4.80382	0.46294
b_1	-1.63146	-0.93499	-0.87473	0.
b_2	1.69924	0.45504	-0.76402	0.
b_3	0.	-1.41345	0.89618	0.18659
b_4	-0.37486	-0.97080	0.31426	0.
b_5	1.89487	1.20349	0.	0.27055
b_{11}	0.	0.15799	0.09588	0.
b_{22}	0.	0	0.	0.
b_{33}	0.	0.22904	-0.19628	0.
b_{44}	-0.26004	0.	0.	0.
b_{55}	-0.19966	0.	0.	0.
b_{12}	0.	0.	0.	0.
b_{13}	0.	-0.11225	-0.11822	-0.32554
b_{14}	0.16743	0.	0.	0.
b_{15}	0.83168	0.	0.19520	0.23157
b_{23}	-0.21038	0.	0.28847	0.
b_{24}	0.	0.10081	0.11330	0.
b_{25}	-0.26114	-0.16424	0.	0.
b_{34}	-0.11924	0.12245	-0.13823	-0.08978
b_{35}	-0.39645	-0.19208	0.12040	0.
b_{45}	0.	0.07725	0.06597	-0.07917

<u>Model Testing.</u>

To use a model for predicting Y on X, variables X and Y should satisfy the model in which the residuals are normally distributed with a mean of 0 and a variance of σ^2 , and the residuals are independent of the X's and the X's are also independent of each other (Dowdy and Wearden, 1983). This can be tested by examining the residuals:

$$R = Y - \hat{Y}$$

where

R is the residual,

Y is the observed value, and

$\hat{Y}$ is the predicted value.

The normality was checked by plotting the residuals versus the observation number for each of the four dependent variables. None of the four plots indicated any lack of normality.

The independence of the residuals was checked by using the runs test. The runs test is designed to test the hypothesis that a sequence of numbers, symbols, or objects is in random order. A run is a sequence of identical numbers, symbols or events precede and followed by different numbers, symbols or events. If there are two possible outcomes such as positive or negative as the residuals in this analysis. If the probability of each outcome keeps constant throughout the process, the expected number of runs is:

$$E(r) = (2N_1N_2)/(N_1+N_2) + 1$$

and

$$\sigma_r = (2N_1N_2(2N_1N_2-N_1-N_2))/(N_1+N_2)^2(N_1+N_2-1)$$

where

N_1 is the number of outcomes of negatives, and
N_2 is the number of outcomes of positive.

The number of runs, r, is approximately normally distributed if either N_1 or N_2 exceeds 20. The approximation is good when both N_1 and N_2 are greater than 10 (Mansfield, 1983).

For each dependent variable, we test the null hypothesis that the runs for the variable are random.

H_0 : Runs are random, $\alpha = .05$

We accept th null hypothesis if

$$E(r) - Z_{\frac{\alpha}{2}}\sigma_r \leq r \leq E(r) + Z_{\frac{\alpha}{2}}\sigma_r$$

The results of each test are listed in Table 6.3. Since number of runs for each dependent variable lies within the expected range of runs, we conclude that there is no evidence of violating the independence of residuals.

Table 6.3. Runs Tests Result

Parameters	Y_1	Y_2	Y_3	Y_4
r	184	181	183	186
N1	196	213	199	211
N2	204	187	201	189
E(r)	200.92	200.155	200.995	200.395
σ_r^2	99.669	98.9	99.744	99.145
σ_r	9.983	9.945	9.987	9.957
Upper limit	220.49	219.64	220.47	219.91
Lower limit	181.36	180.66	181.42	180.88

Chapter 7

Summary and Conclusions

7.1. Summary

To study the effect of ventilation parameters on the dust dispersion across the face area, a literature review on dimensional analysis was carried out. As a result of the review, a one-fifth scale model was constructed with sheet metal. The model was geometrically similar to a real mine opening of 20 by 7.5 ft. The Reynolds number of the air flow was kept the same as that in the coal mine to maintain the kinematic and dynamic similarity.

Two ventilation parameters were included in this study, which were air quantity and line brattice distance. To determine the effects of brattice distance and air quantity on dust dispersion, four brattice distances and air quantities were examined during the study. The experiments utilized both methane gas and Arizona Road Dust for simulating the respirable coal dust. Measurements of methane or dust concentrations and air velocity components were taken at 25 grid points for each brattice distance and air quantity combination. The tests were first carried out without face machines and the same conditions were repeated with the presence of face machines.

For each combination of air quantity and line brattice distance, a substance concentration isopach was plotted to locate the low concentration zone and high concentration spots across the face area. The area of low concentration zone and the change of overall concentration due to the change of ventilation parameters were also summarized. In addition, regression techniques were employed to study the correlation between the substance concentration and ventilation parameters at each grid point as well as that between two substances. Four regression models were constructed to express the relationship between the ventilation parameters and the substance concentration across the face area.

7.2. Conclusions

This study showed that both air quantity increases and brattice extensions are effective in reducing dust concentrations. However, these reductions were not found to be uniform throughout the face. Some points experienced greater reductions than others.

Air quantity increases and brattice extensions tended to have somewhat different effects on dust dispersion patterns. Basically, increases in air quantity were more effective in decreasing concentrations across the face. Brattice extensions were generally more effective in reducing concentrations toward the face.

The presence of face machines changed the flow patterns across the face area. It resulted in reduction of the overall concentration for both substances and, furthermore, shifted the high concentration points toward the open area in front of the return airway. Also, the shape of the low concentration zone became more prominent at the wide side of the face area.

The correlation between the concentration and ventilation parameters differed from point to point. Generally, higher linear correlation showed between the brattice distance and concentration than that of air quantity. And the coefficients between air quantity and concentration were relatively high for the grid point in the return side of airway. Methane correlated well to Road Dust when no face machines were present. With the face machines, better correlations were found at those points closer to the face and in the return side of the airway.

7.3. Recommendations

Either air quantity increases or line brattice extensions can be used to lower dust concentrations. Since air quantity tended to be more effective across the face and brattice extensions were more effective toward the face, the preferred method for reducing dust concentration depends on the location of interest in a face. Consequently, the current air quantity and brattice distance, and also the location of interest should be carefully considered before deciding on the option for dust reduction.

It is recommended that the existence of a low concentration zone be considered and used advantageously in dust control. The ventilation system can be arranged so that the line brattice and the operator compartment of the continuous miner are on the same side of the entry. Another option would be to relocate the operator compartment or position to the tight side. The final recommendation for reducing dust concentrations would be to use dust suppression and/or auxiliary ventilation to dilute the dust concentration at the area where air quantity and brattice extensions are least effective.

BIBLIOGRAPHY

1. AC Spark Plug Div., General Motors Corporation, "Coarse Air Cleaner Test Dust Data Sheet," Batch no. 2515, Detroit, Michigan, undated, 1p.

2. Airco Industrial Gases, "AIRCO Specialty Gases and Equipment," Murray Hill, New Jersey, 1982, 192pp.

3. Breslin, J. A. and Strazisar, A. J., "Dust Control Studies Using Scale Models of Coal Mine Entries and Mining Machines," Bureau of Mines RI 8191, 1976, 20 pp.

4. Combustion Engineering, "Model 8401 Total Hydrocarbon Analyzer Technical Manual," Lewisburg, West Virginia, 1974, 58 pp.

5. Courtney, W. G., "New Developments in Respirable Dust Control," Proc. of 1st Symposium on Underground Mining, Louisville, Kentucky, 1975, pp. 103-109.

6. David, F. W. and Nolle, F. W., "Experimental Modeling in Engineering," Buterworths, Boston, 1982, 185 pp.

7. DAVIS Instrument Manufacturing Company, Inc., "1985-86 CATALOG," Baltimore, Maryland, 1985, 107 pp.

8. Dowdy S., and Wearden, S., "Statistics for Research," John Wiley and Sons, New York, New York, 1983, 537 pp.

9. GCA Corporation, Technology Div., "MODEL RAM-1, REAL-TIME MONITOR INSTRUCTION MANUAL," Bedford, Massachusetts, 1979, 30 pp.

10. Hall, D. A., "The Relation Between Ventilation Airspeed and Respirable Airborne-dust Concentration in Coalmines," Colliery Engineering, Vol. 37, June 1960, pp. 236-239.

11. Hartman, H. L., Mutmansky, J. M., and Wang, Y. J., "Mine Ventilation and Air Conditioning," 2nd ed., John Wiley and Sons, New York, New York, 1982, 791 pp.

12. Johnstone, R. E. and Thring, M. W., "Pilot Plants, Models, and Scale-up Methods in Chemical Engineering," McGraw-Hill, New York, New York, 1957, 307 pp.

13. Luxner, J. V., "Face Ventilation in Underground Bituminous Coal Mines Airflow and Methane Distribution Patterns in Immediate Face Area-Line Brattice," Bureau of Mines RI 7223, 1969, 16 pp.

14. Mansfield, E., "Statistics for Business and Economics Methods and Applications," W. W. Norton and Company, Inc., New York, New York, 1983, 660 pp.

15. Mundell, R. L. and Ondrey, R. S., "Blowing vs. Exhausting Face Ventilation for Respirable Dust Control on Continuous Mining Sections," Proc. of 1st Symposium on Underground Mining, Louisville, Kentucky, 1975, pp. 82-92.

16. Murphy, G., "Similitude in Engineering," Ronald Press, New York, New York, 1951, 166 pp.

17. National Research Council, "Measurement and Control of Respirable Dust in Mines," National Academy of Sciences, Washington, D. C., 1980, 405 pp.

18. Roberson, J. A. and Crown, C. T., "Engineering Fluid Mechanics," 2nd ed., Houghton Mifflin, Boston, Massachusetts, 1980, 661 pp.

19. SAS Institute Inc., "Statistical Analysis System, Version 5," Cary, North Carolina, 1985a.

20. SAS Institute Inc., "SAS User's Guide: Basics, Version 5 Edition," Cary, North Carolina, 1985b, pp. 861-874.

21. SAS Institute Inc., "SAS User's Guide: Statistics, Version 5 Edition," Cary, North Carolina, 1985c, pp. 763-774.

22. Schuring, D. J., Scale Models in Engineering Fundamentals and Applications," Calspan Corporation, Buffalo, New York, 1977, 299 pp.

23. Shuttleworth, S. E. H., "Ventilation at The Face of A Heading, Studies in The Laboratory and Underground," Int. J. Rock Mech. Mining Sci. Vol. 1, 1964, pp. 79-92.

24. Sylvester and Company, "SYLCO FINE POWDER FEEDING APPARATUS, MARK IX, Operating and Maintenance Instructions" Beachwood, Ohio, 1974, 43 pp.

25. Stein, R. L., Breslin, J. A., and Strazisar, A. J., "Investigation of Dust Control by Ventilation Using a Scale Model," Amer. Ind. Hyg. Asso. Jour. Vol 35, Dec. 1974, pp. 815-824.

26. Terrasciences Inc., "SURFACE II, Version 1986," Lakewood, Colorado, 1986.

Appendix A

Scale Modeling Theory and Analysis

A.1. Introduction

The objective of a model study is to predict and determine the conditions under which the performance of a model gives a reliable forecast of prototype performance. The principle of similarity, which deals with the relationships between physical systems of different sizes, is fundamental to the scaling process. It has been shown that mechanical, thermal, or chemical similarity between geometrically similar systems can be specified. This is done through intrinsic ratios of measurements, forces, or rates within each system (Johnstone and Thring, 1957). Since these ratios are of like quantities, they are dimensionless. The first task of any scale model study is to derive and/or adjust the use of these ratios (dimensionless criteria).

In deriving the governing dimensionless criteria, a similarity study is coupled with a method of dimensional analysis; yet logically they are quite distinct. The principle of similarity is a general principle of nature whereas dimensional analysis is one the techniques by which the principle may be applied to specific cases. There are, however, more advantageous approaches to deriving the similarity criteria. For example, using the fundamental differential equations of the model system and governing laws, which dominate the behavior of the model, are two methods preferred by many researchers (Schring, 1977).

A.2. Similarity

Mine ventilation is normally an example of a steady state process in which turbulent flow will nearly always prevail in mine openings (Hartman et al., 1982). The behavior of liberation and movement of respirable mine dust can be considered as an aerodynamic dispersion process (National Science Council, 1980). Two similarity states, geometrical and mechanical, are important in this case.

Geometrical similarity can be defined in terms of correspondence and scale ratio. This means that the flow patterns of the model and the full scale airway must have the same shape. It also means that the ratio between the corresponding linear dimensions in the model and airway must be the same. Therefore, in this study the shape factors for the models will be the same as the real cases, and the scale ratio will be kept constant with respect to the heights, lengths, and widths of airways.

In airflow modeling, mechanical similarity is comprised of kinematic and dynamic features. Kinematic similarity is concerned with a system in motion and dynamic similarity is related to the forces which accelerate or retard moving masses in a dynamic system. These can be regarded as an extension of geometrical similarity concept of stationary or moving systems which are subjected to forces. In fluid systems or systems composed of discrete solid particles, such as the case of coal dust in mine airflow, kinematic similarity necessarily entails dynamic similarity. This is necessary because system motions are functions of the applied forces. Therefore, when the ratios of all corresponding forces are equal, a geometrically similar moving system exists. It is kinematically and dynamically similar.

A.3. Dimensional Analysis of Flow in Airway

Dimensional analysis is a technique for expressing the behavior of a physical system in terms of the minimum number of independent variables and in a form that is unaffected by changes in the magnitude of the units of measurement. The physical quantities are arranged in dimensionless groups consisting of ratios of like quantities (e.g., lengths, velocities, forces, etc.) which characterize the system. These groups constitute the variables in the dimensionless equations of state for the system.

Buckingham's theory is the fundamental theory of dimensional analysis. It states that the solution to every dimensionally homogeneous equation has the form:

$$\varphi(\pi_1, \pi_2, \ldots, \pi_s) = 0 \quad (1)$$

where: π , π , ..., π_s represent the complete set of dimensionless groups of variables and dimensional constants in the equation.

It further states that if an equation contains "n" separate variables, n dimensional constants, and dimensional formulas in terms of m primary quantities; then the number of dimensionless groups in such a complete set is $\pi_s = n - m$ (Murphy, 1950).

From part 1 of Buckingham's theorem, it follows that, when the physical equation relating a given collection of variables is unknown, the arguments π_1, π_2, ..., π_s of the equation in its dimensionless form can be found. This is done by constructing a complete set of dimensionless groups from the variables and any dimensional constants that may be involved. While the form of the function φ and the values of any numerical constants remain undetermined, it is generally not necessary to know these in order to establish conditions of similarity.

Part 2 of Buckingham's theorem shows that, the larger the number of primary quantities m can be made (without causing an increase in n), the smaller the number of dimensionless groups in the complete set. This also results in a dimensional analysis which gives more specific information.

Since the physical laws governing the prototype must prevail in the model, it is helpful to look into the intrinsic properties of the system before actually performing dimensional analysis. For example, the variables, which influence the isothermal flow of a fluid using the MLT system as primary quantities, include linear dimension, fluid velocity, force, density, viscosity, surface tension, and acceleration of gravity. It is obvious that air flow in a mine is turbulent, and the influence of surface tension and the acceleration of gravity are so small that they can be neglected. The usual method of deriving the complete set of dimensionless groups from a given collection of physical variables and dimensional constants is the method of indices. This is an algebraic procedure which was first employed by Rayleigh (David and Nolle, 1982). The variables and dimensional formulas for the airflow problem may include the following:

Variable	Symbol	Dimensional Formula
Linear dimension	L	$[L]$
Air velocity	V	$[L\ T^{-1}]$
Force	F	$[M\ L\ T^{-2}]$
Density	ρ	$[M\ L^{-3}]$
Viscosity	μ	$[M\ L^{-1}\ T^{-1}]$

According to Buckingham's theorem, since n = 5 and m = 3, the expected number of independent dimensionless groups is 5 - 3 = 2.

$$(L, V, F, \rho, \mu) = 0$$

$$(L, V, \rho, \mu) F = 1$$

$$[L]^{\alpha} [V]^{\beta} [\rho]^{\gamma} [\mu]^{\delta} [F] = 0$$

$$[L]^{\alpha}[L\ T^{-1}]^{\beta}[M\ L^{-3}]^{\gamma}[M\ L^{-1}T^{-1}]^{\delta}[M\ L\ T^{-2}] = 0$$

Condition on M: $\gamma + \delta + 1 = 0$

Condition on L: $\alpha + \beta = 3\gamma - \delta + 1 = 0$

Condition on T: $-\beta - \gamma - 2 = 0$

$$[L]^{-1} [V]^{-1} [\rho]^{\gamma} [\mu]^{-\gamma-1} [F] = 0$$

$$[L]^{(\gamma+1)-2}[V]^{(\gamma+1)-2}[\rho]^{(\gamma+1)-1}[\mu]^{-(\gamma+1)}[F] = 0$$

$$\varphi\left(\frac{VL\rho}{\mu}\right) \cdot \frac{F}{\rho V^2 L^2} = 1$$

$$\frac{F}{\rho V^2 L^2} = \varphi\left(\frac{VL\rho}{\mu}\right) \qquad (2)$$

Equation 2 constitutes a complete set of dimensionless groups from the variables listed above, where

$\frac{F}{\rho V^2 L^2}$ = Pressure coefficient

$\frac{VL\rho}{\mu}$ = Reynolds number

A.4. Differential Equations in Airflow Similarity

For most of the modeling processes, the fundamental differential equations are known; the difficulty is often the integration of the equations. The fundamental differential equations for isothermal flow of a Newtonian viscous fluid are the Navier-Stokes equations. Although there is some disagreement as to whether the Navier-Stokes equations can be evolved for turbulent flow, in the case of similarity the general opinion appears to be that parameters evolved for laminar flow can also be applied to turbulent flow (Roberson and Crown, 1980). This can only be done if complete geometrical similarity exists between the systems being considered.

$$\rho \frac{\partial u}{\partial t} + \left(u\frac{\partial u}{\partial x} + v\frac{\partial u}{\partial y} + w\frac{\partial u}{\partial z}\right) = g \cos\alpha_x - \frac{\partial p}{\partial x} + \frac{1}{3}\mu\left(\frac{\partial u}{\partial x} + \frac{\partial v}{\partial y} + \frac{\partial w}{\partial z}\right)$$

I II III IV V

$$+\mu\left(\frac{\partial^2 u}{\partial x^2} + \frac{\partial^2 v}{\partial y^2} + \frac{\partial^2 w}{\partial z^2}\right) \qquad (3)$$

VI

where

ρ is fluid density.

μ is fluid viscosity.

u, v, w are velocity components parallel to the x, y, z axes respectively.

p is pressure.

T is time.

g is acceleration due to gravity acting at an angle α_x to the x axis.

Equation 3 is a dynamic equation in which each term has the dimension of a force. These successive terms are briefly described below:

I. Force required to accelerate a unit mass of fluid when the flow is unsteady.

II. Transport of momentum by fluid flowing through a unit cross-sectional area.

III. Gravitational body force.

IV. Static-pressure gradient.

V. Viscous resistance to a change in the volume of fluid.

VI. Viscous resistance to shear.

The generalized dimensional equation may be written as:

$$[\frac{\rho V}{t}] + [\frac{\rho V^2}{L}] = [\rho g] - [\frac{\Delta P}{L}] + [\frac{\mu V}{L^2}]$$

I II III IV V

In this equation, I and II are dimensionally equivalent. Hence there will be three independent dimensionless groups:

$$\frac{II}{V} = \frac{\rho V L}{\mu} \cdot \frac{II}{III} = \frac{V^2}{Lg} \cdot \frac{IV}{II} = \frac{\Delta P}{\rho V^2}$$

The dimensionless equation may therefore be written as:

$$\varphi(\frac{\rho V L}{\mu} \cdot \frac{V^2}{Lg} \cdot \frac{\Delta P}{\rho V^2}) = \text{Const.}$$

$$\frac{\Delta P}{\rho V^2} = \varphi'(\frac{\rho V L}{\mu} \cdot \frac{V^2}{Lg}) \qquad (4)$$

A.5. Differential equation in Mine Dust Similarity

The differential equations for mass transfer with forced convection are the Navier-Stokes equations together with the mass transfer equation:

$$\underbrace{\left(u\frac{\partial a}{\partial x}+v\frac{\partial a}{\partial y}+w\frac{\partial a}{\partial z}\right)}_{I}+\underbrace{D\left(\frac{\partial^2 a}{\partial x^2}+\frac{\partial^2 a}{\partial y^2}+\frac{\partial^2 a}{\partial z^2}\right)}_{II}=\underbrace{-\frac{\partial a}{\partial t}}_{III} \qquad (5)$$

where

a is concentration of diffusing substance per unit volume.

D is the diffusion coefficient of the diffusing substance.

Successive terms represent:

I: Rate of mass transfer by convection.

II: Rate of mass transfer by diffusion.

III: Rate of change of the concentration.

In dimensional form,

$$\underbrace{\left[\frac{Va}{L}\right]}_{I}+\underbrace{\left[\frac{aD}{L^2}\right]}_{II}=-\underbrace{\left[\frac{a}{t}\right]}_{III}$$

Terms I and III are dimensionally equivalent; hence, there is one dimensionless group which may be written for the steady state:

$$\varphi\left(\frac{VL}{D}\right) = \text{Const.}$$

(6)

If Equation 5, which was derived from the Navier-Stokes equations, is combined with the dimensionless equation for the steady state, we obtained

$$\varphi\left(\frac{\rho VL}{\mu} \cdot \frac{V^2}{Lg} \cdot \frac{\Delta P}{\rho V^2} \cdot \frac{VL}{D}\right) = \text{Const.}$$

or

$$\varphi\left(\frac{\rho VL}{\mu} \cdot \frac{V^2}{Lg} \cdot \frac{\Delta P}{\rho V^2} \cdot \frac{\mu}{\rho D}\right) = \text{Const.}$$

where: $\frac{\mu}{\rho D}$ is the Schmidt group.

A.6. Discussion

Based on the dimensional analysis, the Navier-Stokes equations of flow, and the diffusion equation, the scaling problem in this study must satisfy the following dimensionless groups:

$\frac{\rho VL}{\mu}$	Reynolds number (ratio of inertial to viscous forces)
$\frac{V^2}{g}$	Froude group (ratio of inertial to gravitational forces)
$\frac{\mu}{\rho D}$	Schmidt group (ratio of kinematic viscosity

to diffusivity)

Actually, if surface tension forces are considered in the dimensional analysis, the Weber group (the ratio of inertial to surface tension forces) should be taken into consideration. It is obvious that the Reynolds number, the Froude group, and the Weber group are mutually incompatible, since each one requires the fluid velocity to vary as a different function of the linear dimension. For the model design requirement, it is advantageous to choose conditions such that the rate of the whole process depends predominantly upon one dimensionless criterion. Basically, the airflow in the mine openings is usually turbulent, with Reynolds number ranging from 0.5×10^4 to 20×10^4. Under this condition, gravitational and surface tension forces are relatively unimportant. Therefore, it is reasonable to maintain the same value of Reynolds number for the model and actual mine airways.

Theoretically, when the mine airway is scaled down to the model size, in order to be geometrically similar, the diameter of respirable mine dust should also be consistently scaled down by the same factor. As described before, the similarity of the mine dust and the airflow is governed by the criteria of the Reynolds number and Schmidt group. The Schmidt group is defined as the ratio of kinematic viscosity to the diffusion coefficient of the diffusing substance. This only describes the physical properties of the fluid. Hence, for this study, the Schmidt number is assumed to be a constant. In cases where the Reynolds number is kept the same for both the model and the prototype, the dynamic behavior of the respirable mine dust should be preserved. Because a point to point geometrical correspondence between two systems ensures that if the overall values of the intrinsic ratio (i.e., Reynolds number) are equal, the corresponding point values will be equal throughout.

A.7. Conclusions

The following conclusions can be drawn from this similarity and dimensional analysis:

1. The airflow modeling should employ Reynolds number criterion. That is

   $$V_{model} = kV_{mine}$$

   where V and k are the velocity and the scale ratio, respectively.

2. The dynamic behavior of respirable mine dust can be preserved by keeping the same Reynolds number in the model.

APPENDIX B

CONCENTRATION DATA

Table B.1. Methane Concentration Without Face Machines at 4 ft Brattice Distance

Grid Point	Air Quantity, in cfm			
	3400	2400	1800	1000
1	539	1124	1204	848
2	1789	2351	2661	4275
3	2167	3314	3979	4275
4	2878	3635	4874	8050
5	4163	3899	4805	7443
6	2202	3268	2752	7051
7	1823	2683	2993	4391
8	1445	1778	2282	4213
9	264	619	711	1374
10	30	30	30	30
11	30	30	30	30
12	30	115	149	178
13	940	1170	1411	1606
14	1193	1445	1812	2713
15	1445	2259	2271	3231
16	860	1342	1502	3356
17	803	963	1433	1999
18	631	883	1055	964
19	92	252	241	411
20	172	229	344	500
21	172	206	229	303
22	275	310	356	464
23	367	447	516	741
24	539	654	745	1767
25	631	700	975	1535

Table B.2. Methane Concentration Without Face Machines at 3 ft Brattice Distance

Grid Point	Air Quantity, in cfm			
	3400	2400	1800	1000
1	30	30	30	73
2	218	382	424	158
3	1525	1899	3134	3914
4	1617	2002	3016	4730
5	1697	2212	3734	3146
6	1135	1077	1708	1768
7	998	1227	2238	2134
8	161	208	271	451
9	30	30	30	61
10	30	30	30	30
11	30	30	30	30
12	30	30	30	30
13	30	30	60	85
14	585	868	1437	1122
15	1376	973	2556	2938
16	1158	1563	2358	4316
17	482	903	1001	646
18	30	93	471	110
19	183	289	353	585
20	183	289	365	610
21	30	139	82	268
22	264	197	200	402
23	206	301	292	638
24	344	602	695	1573
25	1112	1436	1447	3438

Table B.3. Methane Concentration Without Face Machines at 2 ft Brattice Distance

Grid Point	Air Quantity, in cfm			
	3400	2400	1800	1000
1	30	30	30	30
2	30	30	30	30
3	275	378	1296	1002
4	631	677	2352	2416
5	677	596	2480	2222
6	287	654	1088	1244
7	218	281	864	743
8	30	30	30	30
9	30	30	30	30
10	30	30	30	30
11	30	30	30	30
12	30	30	30	30
13	30	30	30	30
14	30	30	256	170
15	2821	3521	6113	7818
16	2729	2397	4504	5521
17	115	132	464	517
18	172	178	560	565
19	149	172	592	574
20	183	183	608	609
21	30	115	256	252
22	126	30	252	264
23	275	378	288	557
24	872	1112	2256	1572
25	2328	3028	5912	5884

Table B.4. Methane Concentration Without Face Machines at 1 ft Brattice Distance

Grid Point	Air Quantity, in cfm			
	3400	2400	1800	1000
1	30	30	30	30
2	30	30	30	30
3	30	30	30	30
4	30	68	161	321
5	30	72	298	298
6	30	68	333	1904
7	30	30	30	80
8	30	30	30	80
9	30	30	30	97
10	30	30	30	92
11	30	30	30	103
12	30	30	30	103
13	30	30	30	97
14	30	30	30	30
15	30	30	30	161
16	30	30	103	562
17	30	123	172	298
18	76	127	206	333
19	87	119	195	310
20	108	159	240	367
21	531	775	768	975
22	686	1034	1021	1319
23	787	1105	1525	1835
24	924	1165	1835	2821
25	1851	2248	5241	4794

Table B.5. Methane Concentration With Face Machines at 4 ft Brattice Distance

Grid Point	Air Quantity, in cfm			
	3400	2400	1800	1000
1	30	30	92	110
2	30	30	62	106
3	200	133	167	177
4	260	213	288	360
5	110	100	106	158
6	125	123	202	234
7	170	103	118	217
8	65	35	86	121
9	45	30	69	83
10	30	49	108	89
11	30	55	81	83
12	30	30	82	95
13	110	153	608	1540
14	620	560	743	830
15	95	77	216	246
16	260	319	814	1115
17	680	606	1195	1792
18	470	167	1234	1540
19	70	71	139	156
20	230	223	423	419
21	80	49	172	276
22	55	71	424	524
23	120	139	692	863
24	275	345	801	1188
25	335	413	900	1148

Table B.6. Methane Concentration With Face Machines at 3 ft Brattice Distance

Grid Point	Air Quantity, in cfm			
	3400	2400	1800	1000
1	60	88	87	113
2	54	82	99	105
3	59	84	89	98
4	42	74	79	101
5	48	61	72	59
6	55	83	65	70
7	46	82	79	79
8	45	68	77	79
9	53	80	98	95
10	62	80	103	119
11	47	79	93	122
12	50	77	81	101
13	43	55	96	112
14	112	151	239	286
15	62	80	102	89
16	45	78	101	218
17	376	453	430	573
18	147	111	109	243
19	131	245	332	402
20	145	296	426	525
21	143	165	121	167
22	58	104	93	216
23	75	166	135	266
24	60	134	259	432
25	60	117	243	450

Table B.7. Methane Concentration With Face Machines at 2 ft Brattice Distance

Grid Point	Air Quantity, in cfm			
	3400	2400	1800	1000
1	90	85	105	116
2	105	85	110	135
3	45	30	80	90
4	60	30	70	100
5	60	38	65	100
6	60	45	85	90
7	60	30	68	87
8	45	85	90	82
9	105	80	90	130
10	97	85	105	110
11	90	90	110	150
12	120	85	125	125
13	45	90	75	90
14	60	40	70	105
15	60	52	100	73
16	60	54	110	85
17	75	180	397	545
18	210	226	210	280
19	277	260	270	348
20	270	310	310	415
21	210	230	235	336
22.	135	197	215	300
23	120	109	160	248
24	60	45	95	268
25	60	60	105	136

Table B.8. Methane Concentration With Face Machines at 1 ft Brattice Distance

Grid Point	Air Quantity, in cfm			
	3400	2400	1800	1000
1	30	30	40	45
2	30	30	60	60
3	30	30	30	70
4	90	30	35	80
5	50	30	32	40
6	30	30	49	55
7	40	30	38	30
8	30	30	45	90
9	30	30	50	60
10	30	30	40	66
11	30	30	40	64
12	30	30	45	67
13	30	30	37	60
14	45	30	45	40
15	40	30	45	50
16	30	30	45	40
17	130	105	192	520
18	90	85	170	678
19	95	100	215	600
20	115	125	235	570
21	110	160	270	570
22	50	65	155	525
23	30	30	40	375
24	30	30	55	90
25	35	30	60	60

Table B.9. Dust Concentration Without Face Machines at 4 ft Brattice Distance

Grid Point	Air Quantity, in cfm			
	3400	2400	1800	1000
1	7.40	10.64	26.56	12.35
2	21.78	31.92	38.43	30.15
3	25.21	38.92	53.68	93.90
4	27.51	45.64	57.64	99.33
5	35.53	45.92	94.33	120.87
6	22.92	38.64	72.30	120.87
7	18.34	31.92	42.38	74.13
8	17.19	21.56	29.38	35.58
9	4.48	5.88	16.39	12.56
10	0.95	1.96	2.19	1.37
11	0.71	0.84	2.41	1.37
12	1.21	0.42	4.43	5.16
13	5.83	11.20	25.43	19.27
14	7.51	9.52	28.25	36.08
15	11.60	25.20	94.33	106.25
16	37.82	42.56	92.64	104.77
17	6.83	7.00	21.47	21.18
18	4.10	7.84	18.08	18.78
19	0.53	2.24	8.42	7.85
20	0.74	4.06	9.14	4.17
21	0.45	1.23	5.27	2.30
22	0.82	2.80	9.21	11.08
23	4.52	5.60	12.43	12.35
24	7.88	6.72	16.95	16.80
25	13.13	8.96	22.03	23.23

Table B.10. Dust Concentration Without Face Machines at 3 ft Brattice Distance

Grid Point	Air Quantity, in cfm			
	3400	2400	1800	1000
1	1.40	1.95	1.67	0.50
2	11.46	7.56	18.60	12.88
3	31.63	3.84	36.96	49.28
4	38.41	58.24	59.36	96.88
5	35.59	52.08	64.96	97.52
6	15.82	20.16	28.56	29.12
7	18.60	30.80	36.40	47.32
8	3.82	4.89	11.18	5.50
9	1.91	1.23	1.39	0.44
10	1.51	1.00	1.11	0.44
11	0.89	1.20	0.77	0.39
12	1.63	1.11	1.56	0.50
13	1.97	1.72	2.61	1.50
14	8.99	12.40	16.80	12.32
15	10.95	11.76	14.56	31.92
16	29.37	39.76	60.88	85.40
17	7.75	10.73	12.32	15.12
18	3.10	3.28	5.34	6.00
19	4.45	4.28	6.95	6.67
20	4.17	4.17	5.84	7.78
21	5.84	4.84	1.33	2.22
22	1.07	1.44	2.50	4.33
23	6.31	4.11	5.45	7.78
24	5.90	5.28	6.39	16.80
25	19.20	5.78	24.08	27.44

Table B.11. Dust Concentration Without Face Machines at 2 ft Brattice Distance

Grid Point	Air Quantity, in cfm			
	3400	2400	1800	1000
1	1.27	1.43	1.08	0.53
2	1.67	1.55	1.13	0.56
3	3.39	14.00	11.76	45.40
4	12.68	15.68	24.08	83.40
5	6.23	9.01	20.72	48.70
6	7.01	7.78	6.12	9.78
7	5.06	3.39	7.34	22.40
8	0.94	0.98	0.78	0.53
9	1.56	1.33	1.08	0.50
10	1.16	1.36	0.32	0.56
11	1.33	1.19	1.08	0.30
12	1.09	1.37	1.08	0.56
13	0.39	1.15	1.28	0.78
14	1.67	1.56	3.00	1.61
15	2.89	32.48	109.76	118.72
16	40.88	44.80	87.36	147.28
17	1.95	1.61	4.06	5.00
18	3.06	4.11	4.28	9.25
19	3.67	3.89	3.84	10.53
20	3.67	4.06	3.61	7.09
21	0.76	0.56	1.39	1.75
22	0.89	0.72	0.76	2.58
23	1.00	1.95	1.11	2.80
24	6.16	6.73	8.12	5.56
25	21.28	27.44	29.12	11.12

Table B.12. Dust Concentration Without Face Machines at 1 ft Brattice Distance

Grid Point	Air Quantity, in cfm			
	3400	2400	1800	1000
1	2.75	2.44	1.45	1.43
2	2.97	1.50	1.95	1.35
3	3.28	2.11	1.67	0.97
4	4.34	3.89	21.84	19.60
5	2.00	2.78	2.89	10.45
6	2.89	2.94	4.11	112.00
7	4.61	2.44	7.23	1.43
8	3.39	2.11	1.19	1.54
9	2.94	2.27	1.46	0.69
10	2.70	2.14	1.47	1.70
11	1.92	2.50	2.28	1.52
12	2.33	1.89	1.95	1.47
13	2.06	1.16	1.28	1.73
14	3.22	2.22	5.34	1.23
15	2.95	10.06	25.20	43.12
16	6.06	30.80	51.52	35.84
17	6.84	5.34	11.73	7.51
18	3.70	5.22	6.84	8.51
19	4.17	4.33	6.51	7.56
20	5.14	4.33	6.06	9.90
21	3.06	2.72	4.17	5.78
22	1.97	3.06	5.89	4.78
23	3.22	3.11	5.28	8.95
24	10.01	11.73	24.08	19.60
25	38.08	49.84	50.96	36.96

Table B.13. Dust Concentration With Face Machines at 4 ft Brattice Distance

Grid Point	Air Quantity, in cfm			
	3400	2400	1800	1000
1	0.56	0.78	0.56	1.00
2	0.56	0.72	0.72	1.39
3	1.11	0.67	1.72	1.50
4	1.84	1.33	3.00	4.84
5	1.56	1.39	1.39	2.06
6	1.17	2.17	2.39	2.61
7	1.83	1.89	2.11	2.89
8	0.78	0.50	1.00	0.50
9	0.50	0.56	0.72	1.28
10	0.50	0.67	0.56	1.56
11	0.50	0.50	0.50	0.94
12	0.50	0.50	0.61	0.50
13	2.56	2.39	8.51	14.07
14	7.51	13.90	17.24	19.46
15	1.45	1.89	3.06	9.34
16	58.38	150.12	125.66	103.42
17	9.73	10.79	22.24	34.47
18	5.95	2.72	16.96	21.68
19	0.56	0.50	0.56	0.72
20	3.28	1.61	6.06	7.78
21	0.67	0.50	1.11	3.22
22	0.89	1.22	3.22	1.22
23	2.06	1.39	6.84	12.79
24	4.28	7.95	15.17	19.46
25	6.67	10.79	16.40	22.80

Table B.14. Dust Concentration With Face Machines at 3 ft Brattice Distance

Grid Point	Air Quantity, in cfm			
	3400	2400	1800	1000
1	0.72	0.50	1.22	1.11
2	0.67	0.50	1.33	1.28
3	0.78	0.61	0.94	1.67
4	0.89	0.83	2.61	3.78
5	0.67	0.89	1.11	1.11
6	0.61	1.00	1.72	2.33
7	1.11	1.17	3.78	5.67
8	0.56	0.50	0.61	1.67
9	0.56	0.50	1.11	1.11
10	0.50	0.50	1.39	0.83
11	0.56	0.68	1.44	1.06
12	0.61	0.68	1.00	0.72
13	0.50	0.50	0.72	5.17
14	3.00	3.61	7.06	12.12
15	0.56	1.00	1.67	1.22
16	1.61	1.45	42.00	268.80
17	4.17	5.06	6.78	13.73
18	0.61	0.89	0.94	5.23
19	2.28	2.78	5.78	6.06
20	3.34	5.34	6.23	7.01
21	2.17	2.06	1.78	2.39
22	0.56	1.17	0.50	2.95
23	1.00	2.84	2.17	4.00
24	7.45	10.01	6.45	9.90
25	36.40	48.72	38.08	9.12

Table B.15. Dust Concentration With Face Machines at 2 ft Brattice Distance

Grid Point	Air Quantity, in cfm			
	3400	2400	1800	1000
1	0.94	0.50	0.50	0.50
2	1.11	0.50	0.50	0.50
3	1.11	0.50	0.50	0.83
4	1.39	0.50	0.50	1.33
5	0.67	1.11	0.94	1.78
6	0.67	0.83	1.28	1.95
7	1.00	0.56	0.50	1.17
8	0.89	0.50	0.50	0.72
9	0.67	0.56	0.50	0.89
10	0.89	0.50	0.50	0.61
11	0.56	0.50	0.50	0.56
12	0.61	0.56	0.50	0.50
13	0.61	0.50	0.50	0.61
14	0.67	0.61	0.50	2.56
15	0.56	1.00	1.39	3.17
16	0.94	58.80	56.56	3.06
17	1.11	3.06	2.61	7.23
18	2.17	1.89	1.83	4.45
19	3.06	2.00	1.11	3.45
20	1.39	0.83	0.56	4.45
21	0.61	0.50	0.50	4.56
22	0.56	1.06	1.56	3.17
23	0.78	0.72	1.06	1.28
24	1.50	0.56	0.56	4.00
25	6.12	4.48	1.17	4.00

Table B.16. Dust Concentration With Face Machines at 1 ft Brattice Distance

Grid Point	Air Quantity, in cfm			
	3400	2400	1800	1000
1	0.53	0.89	0.89	0.56
2	0.53	1.01	0.61	0.50
3	0.64	0.89	1.06	0.39
4	0.71	1.00	0.94	1.00
5	0.71	1.39	1.61	1.22
6	0.75	1.45	1.39	1.67
7	0.71	1.06	0.89	0.61
8	0.68	0.83	0.89	0.56
9	0.53	1.11	0.83	0.50
10	0.50	0.78	0.77	0.56
11	0.50	0.72	0.67	0.50
12	0.50	0.89	0.94	0.56
13	0.50	0.72	0.78	0.61
14	0.53	1.11	1.11	0.50
15	0.53	0.94	1.17	1.72
16	1.07	1.17	1.61	1.45
17	4.17	1.78	1.89	3.28
18	4.06	3.28	3.89	2.84
19	1.17	1.89	1.89	1.33
20	1.39	1.83	1.78	1.11
21	2.11	2.50	2.67	1.67
22	1.11	2.89	3.34	1.61
23	6.06	2.45	1.28	1.83
24	2.67	1.89	0.56	1.33
25	19.04	4.17	1.72	0.83

APPENDIX C

METHANE AND DUST CONCENTRATION ZONE

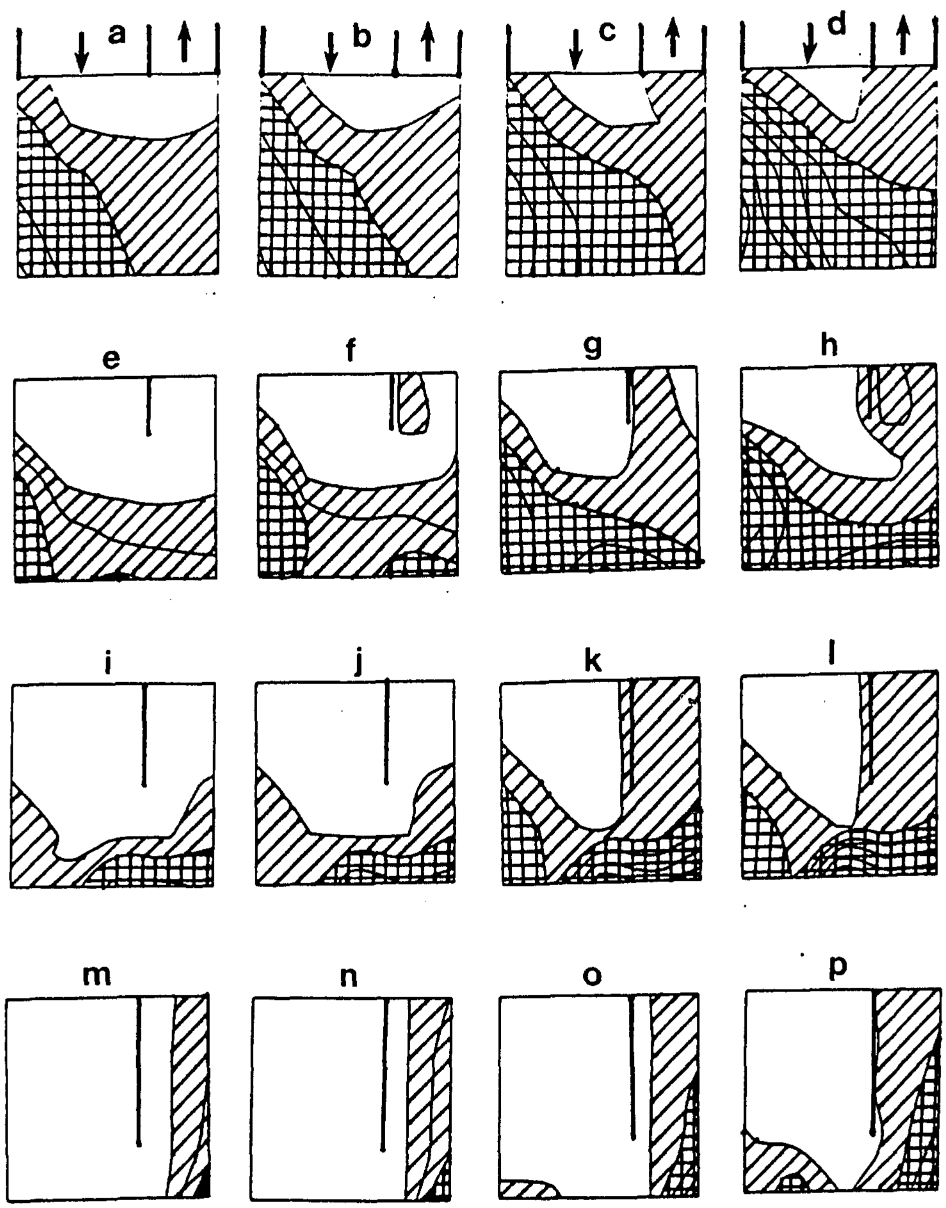

(a) B=4, Q=3400 (b) B=4, Q=2400 (c) B=4, Q=1800 (d) B=4, Q=1000
(e) B=3, Q=3400 (f) B=3, Q=2400 (g) B=3, Q=1800 (h) B=3, Q=1000
(i) B=2, Q=3400 (j) B=2, Q=2400 (k) B=2, Q=1800 (l) B=2, Q=1000
(m) B=1, Q=3400 (n) B=1, Q=2400 (o) B=1, Q=1800 (p) B=1, Q=1000
B: Brattice distance, in ft; Q: Air quantity, in cfm.

Fig. C.1. Methane Concentration Without Face Machines

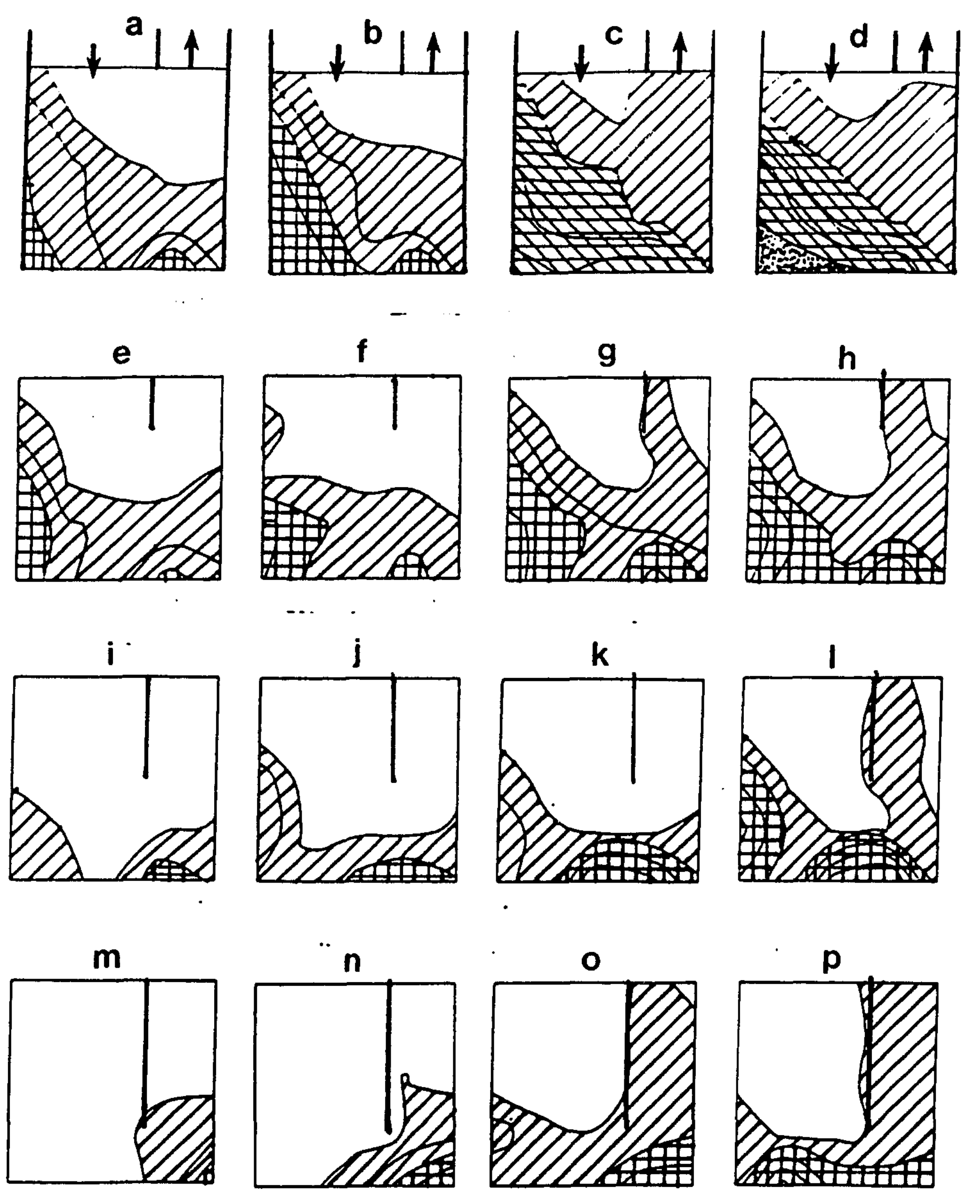

(a) B=4, Q=3400 (b) B=4, Q=2400 (c) B=4, Q=1800 (d) B=4, Q=1000
(e) B=3, Q=3400 (f) B=3, Q=2400 (g) B=3, Q=1800 (h) B=3, Q=1000
(i) B=2, Q=3400 (j) B=2, Q=2400 (k) B=2, Q=1800 (l) B=2, Q=1000
(m) B=1, Q=3400 (n) B=1, Q=2400 (o) B=1, Q=1800 (p) B=1, Q=1000
B: Brattice distance, in ft; Q: Air quantity, in cfm.

Fig. C.2. Dust Concentration Without Face Machines

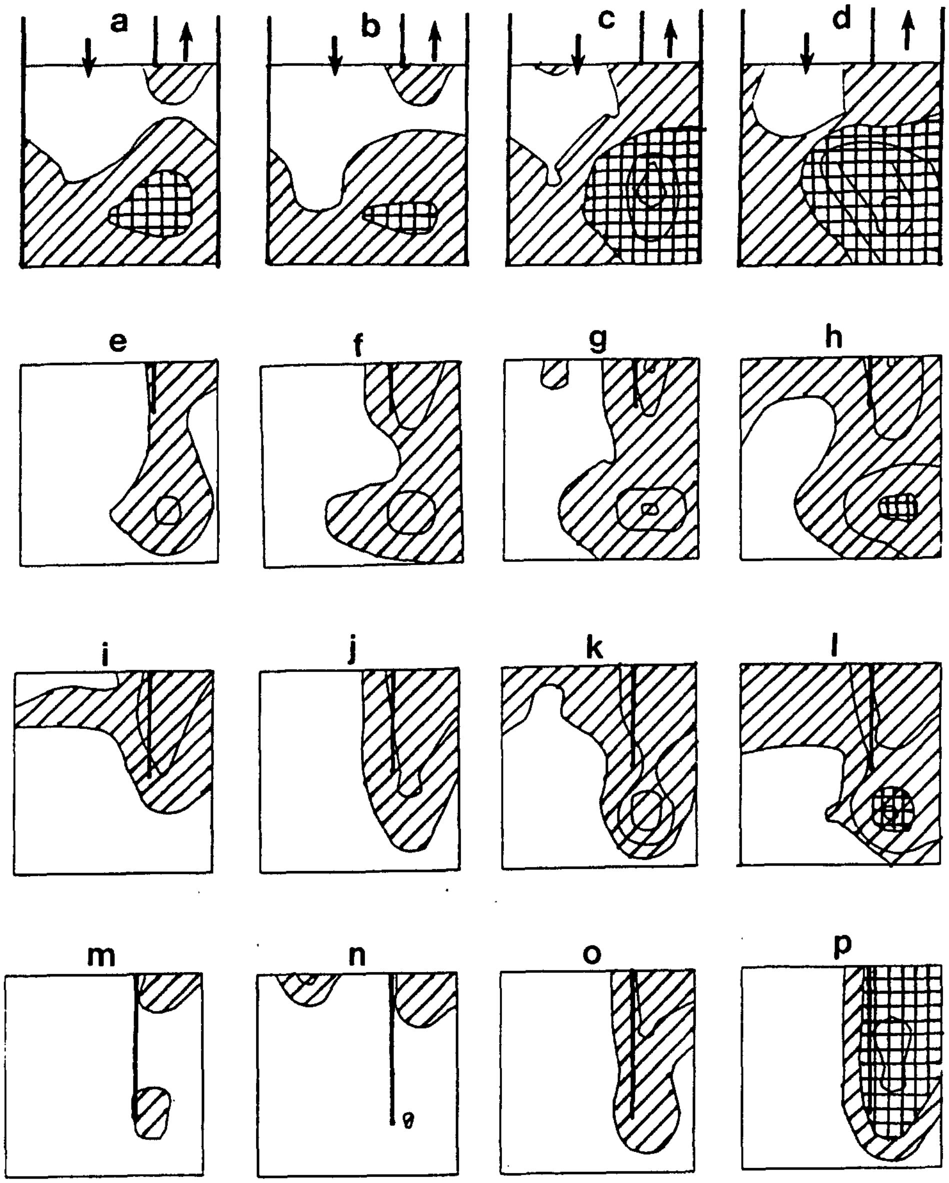

(a) B=4, Q=3400 (b) B=4, Q=2400 (c) B=4, Q=1800 (d) B=4, Q=1000
(e) B=3, Q=3400 (f) B=3, Q=2400 (g) B=3, Q=1800 (h) B=3, Q=1000
(i) B=2, Q=3400 (j) B=2, Q=2400 (k) B=2, Q=1800 (l) B=2, Q=1000
(m) B=1, Q=3400 (n) B=1, Q=2400 (o) B=1, Q=1800 (p) B=1, Q=1000
B: Brattice distance, in ft; Q: Air quantity, in cfm.

Fig. C.3. Methane Concentration with Face Machines

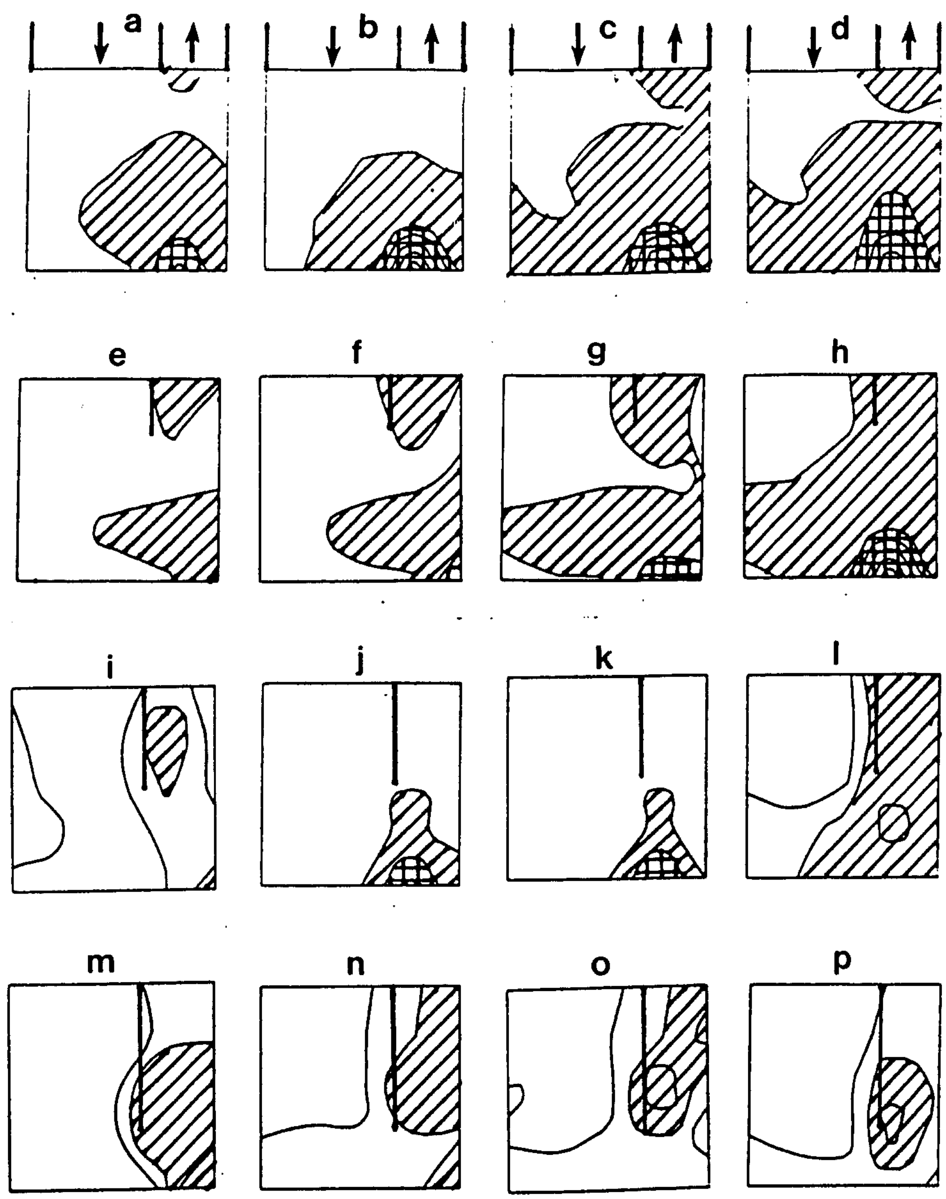

(a) B=4, Q=3400 (b) B=4, Q=2400 (c) B=4, Q=1800 (d) B=4, Q=1000
(e) B=3, Q=3400 (f) B=3, Q=2400 (g) B=3, Q=1800 (h) B=3, Q=1000
(i) B=2, Q=3400 (j) B=2, Q=2400 (k) B=2, Q=1800 (l) B=2, Q=1000
(m) B=1, Q=3400 (n) B=1, Q=2400 (o) B=1, Q=1800 (p) B=1, Q=1000
B: Brattice distance, in ft; Q: Air quantity, in cfm.

Fig. C.4. Dust Concentration with Face Machines

VITA

Tzuu Hsing Ueng was born in Taiwan, on February 26, 1953. He received his B.S.M.E. degree from National Cheng Kung University, Taiwan, in 1975. After completing his military service he worked as a project engineer for two years. In 1979, he came to the United States to pursue his graduate study at West Virginia University. He received his M.S. degree in Mining Engineering in 1982 from West Virginia University.

APPROVAL OF EXAMINING COMMITTEE

Robert N. Eli, Civil Engineering

Wafik H. Iskander, Industrial Engineering

Syd S. Peng, Mining Engineering

Ronald R. Rollins, Mining Engineering

May 18, 1988
Date

Yih J. Wang, Mining Engineering, Chairman